

Aus dem Zentrum für Augenheilkunde
der Universität zu Köln
Direktor: Universitätsprofessor Dr. med. C. Cursiefen

Comparative Proteomic Analysis of Regenerative and Degenerated Mouse Retinas

Inaugural-Dissertation zur Erlangung der Doktorwürde
der Medizinischen Fakultät
der Universität zu Köln

vorgelegt von
Xiaosha Wang
aus Anhui, China

promoviert am 10. Juli 2025

Gedruckt mit Genehmigung der Medizinischen Fakultät der Universität zu Köln
Druckjahr: 2025

Dekan: Universitätsprofessor Dr. med. G. R. Fink

1. Gutachterin: Universitätsprofessorin Dr. med. V. Prokoch

2. Gutachter: Universitätsprofessor Dr. M. Bergami

Erklärung

Ich erkläre hiermit, dass ich die vorliegende Dissertationsschrift ohne unzulässige Hilfe Dritter und ohne Benutzung anderer als der angegebenen Hilfsmittel angefertigt habe; die aus fremden Quellen direkt oder indirekt übernommenen Gedanken sind als solche kenntlich gemacht.

Bei der Auswahl und Auswertung des Materials sowie bei der Herstellung des Manuskriptes habe ich keine Unterstützungsleistungen von folgenden Personen erhalten: Universitätsprofessor Dr. med. Verena Prokoch und Dr. med. Hanhan Liu.

Weitere Personen waren an der Erstellung der vorliegenden Arbeit nicht beteiligt. Insbesondere habe ich nicht die Hilfe einer Promotionsberaterin/eines Promotionsberaters in Anspruch genommen. Dritte haben von mir weder unmittelbar noch mittelbar geldwerte Leistungen für Arbeiten erhalten, die im Zusammenhang mit dem Inhalt der vorgelegten Dissertationsschrift stehen.

Die Dissertationsschrift wurde von mir bisher weder im Inland noch im Ausland in gleicher oder ähnlicher Form einer anderen Prüfungsbehörde vorgelegt.

Die in dieser Arbeit angegebenen Experimente sind nach entsprechender Anleitung durch Frau Universitätsprofessor Dr. med. Verena Prokosch und Frau Dr. Hanhan Liu von mir selbst ausgeführt worden.

Die Tierversuche wurden in Zusammenarbeit mit Dr. med. Maoren Wang, Dr. med. Hanhan Liu, Dr. med. Panpan Li und Dr. med. Yuan Feng erfolgreich durchgeführt. Die Probenvorbereitung für die Proteomik wurde von Frau Layla Fröhn und mir übernommen, während die Probenanalyse in der CECAD/CMMC Proteomics Core Facility erfolgte. Alle anderen Experimente und Analysen habe ich selbst durchgeführt.

Erklärung zur guten wissenschaftlichen Praxis:

Ich erkläre hiermit, dass ich die Ordnung zur Sicherung guter wissenschaftlicher Praxis und zum Umgang mit wissenschaftlichem Fehlverhalten (Amtliche Mitteilung der Universität zu Köln AM 132/2020) der Universität zu Köln gelesen habe und verpflichte mich hiermit, die dort genannten Vorgaben bei allen wissenschaftlichen Tätigkeiten zu beachten und umzusetzen.

Köln, den 12.02.2025

Unterschrift:

ACKNOWLEDGEMENTS

I would like to extend my deepest gratitude to my supervisor, Univ.-Prof. Dr. med. Verena Prokosch, for her invaluable guidance and sustained support throughout this project. Her encouragement and trust have not only propelled my academic growth but have also helped me navigate the personal challenges of my scientific journey.

Special thanks to Dr. Hanhan Liu for her generous assistance and expert advice, which were crucial to the successful implementation of my project. I am also grateful to my colleagues in our research group—Layla Frühn, Dr. Panpan Li, Dr. Yuan Feng, Dr. Xin Shi, and Dr. Julia Prinz—for their collaboration and support.

Additionally, I must express my heartfelt appreciation to my friends, who stood by me during tough times and celebrated my achievements. Their unwavering presence has been a constant source of comfort and joy.

I am also deeply grateful to my family. Despite the physical distance between us, their open-mindedness and encouragement have enabled me to pursue my passions without burden. Their continual support and love have been my constant source of strength.

Dedication

To my beloved families and friends

TABLE OF CONTENTS

ABBREVIATION	7
1. SUMMARY	8
2. DEUTSCHE ZUSSAMENFASSUNG	9
3. INTRODUCTION	10
3.1. Glaucoma	10
3.1.1. Epidemiology of Glaucoma	10
3.1.2. Pathophysiology of Glaucoma	10
3.1.3. Limitations of Current Treatments	10
3.2. Current Research on Pathways in Axonal Regeneration	12
3.2.1. Intrinsic Pathways	12
3.2.2. Extrinsic Pathways	12
3.2.3. Limitations of Recent Research on Retinal Ganglion Cell Axonal Regeneration	13
3.3. Proteomics	14
3.3.1. Overview of Proteomics	14
3.3.2. Data-Independent Acquisition Mass Spectrometry (DIA-MS)	14
3.4. Aims of the Work	16
4. PUBLICATION	17
5. DISCUSSION	34
5.1. Proteomic Characteristic in Regenerative Retina	34
5.1.1. Thyroid Hormone Signaling Pathway	34
5.1.2. Wnt and Notch Signaling Pathways	34
5.1.3. SIRT1/ CaMKII α / CBP / EP300 as Key Players	35
5.2. Proteomic Characteristic in Glaucomatous Degenerative Retina	37
5.2.1. Pathways of Neurodegeneration	37
5.2.2. Apoptotic Signaling Pathway in Response to Endoplasmic Reticulum (ER) Stress	37
5.2.3. Cytoplasmic Stress Granule	37
5.2.4. Mitochondrial Functions	38

6.	REFERENCES	39
7.	PRE-PUBLICATION OF RESULTS	45

ABBREVIATION

ASK1	Apoptosis signal-regulating kinase 1
CBP	Histone lysine acetyltransferase CREBBP
CNS	Central nervous system
CSAP9	Caspase-9
DDA	Data-dependent acquisition
DIA-MS	Data-independent acquisition mass spectrometry
EP300	Histone acetyltransferase p300
ER	Endoplasmic reticulum
IOP	Intraocular pressure
ITPR1	Inositol 1,4,5-trisphosphate receptor type 1
MAP3K5	Mitogen-activated protein kinase kinase kinase 5
MS	Mass spectrometry
NTG	Normal-tension glaucoma
RGC	Retinal ganglion cell
SG	Stress granule
SIRT1	NAD-dependent protein deacetylase sirtuin-1

1. SUMMARY

In this study, we utilized retinal ganglion cell (RGC) degeneration and regeneration models along with DIA-MS to investigate proteomic alterations during these processes. Collaborative up-regulated signaling pathways involving thyroid hormone, Notch, and Wnt were observed during RGC regeneration, with key players such as SIR1, CBP, EP300, and CaMKII α identified. Furthermore, critical molecular players, including ITPR1, M3K5, CIO72 and CASP9, were identified as up-regulated in degenerated retinas. This research provides insight into the molecular mechanisms underlying glaucomatous RGC degeneration and regeneration. Future studies should further investigate the identified pathways, proteins, and their interactions developing therapeutic strategies to protect and regenerate RGCs in glaucoma and other neurodegenerative conditions. Understanding these processes is crucial for advancing the knowledge of vision loss and potential treatments to improve treatment strategies in glaucoma.

2. DEUTSCHE ZUSAMMENFASSUNG

In dieser Studie haben wir Modelle zur Degeneration und Regeneration retinaler Ganglienzellen (RGC) zusammen mit DIA-MS verwendet, um proteomische Veränderungen während dieser Prozesse zu untersuchen. Während der RGC-Regeneration wurden gemeinsame hochregulierte Signalwege unter Beteiligung von Schilddrüsenhormon, Notch und Wnt beobachtet, wobei Schlüsselakteure wie SIR1, CBP, EP300 und CaMKII α identifiziert wurden. Darüber hinaus wurde festgestellt, dass wichtige molekulare Akteure, darunter ITPR1, M3K5, CIO72 und CASP9, in degenerierten Netzhäuten hochreguliert sind. Diese Forschungsarbeit gibt Aufschluss über die molekularen Mechanismen, die der Degeneration und Regeneration glaukomatöser RGC zugrunde liegen. Künftige Studien sollten die identifizierten Signalwege, Proteine und ihre Wechselwirkungen weiter untersuchen, um therapeutische Strategien zum Schutz und zur Regeneration von RGCs bei Glaukom und anderen neurodegenerativen Erkrankungen zu entwickeln. Das Verständnis dieser Prozesse ist von entscheidender Bedeutung, um das Wissen über Sehkraftverlust und potenzielle Behandlungen zu erweitern und somit die Therapieansätze für das Glaukom zu verbessern.

3. INTRODUCTION

3.1 Glaucoma

3.1.1 Epidemiology of Glaucoma

Glaucoma is a major cause of irreversible blindness worldwide [1]. In 2020, the global prevalence of glaucoma was estimated at approximately 80 million individuals, a figure projected to increase to 112 million by 2040 due to the aging global population [2]. Notably, 3-4% of individuals diagnosed with glaucoma may progress to complete blindness if left untreated [3]. Since the disease is typically asymptomatic in its early stages, many cases go undetected until significant optic nerve damage has occurred, resulting in permanent vision loss [4]. This silent progression makes glaucoma a critical public health issue worldwide [5].

3.1.2 Pathophysiology of Glaucoma

Glaucoma is a chronic, progressive neurodegenerative disease characterized by retinal ganglion cell (RGC) loss and optic nerve damage, resulting in irreversible vision loss [1, 4]. Its pathophysiology primarily involves elevated intraocular pressure (IOP) and optic nerve damage [4]. Elevated IOP, typically caused by impaired aqueous humor outflow through the trabecular meshwork, induces mechanical deformation of the optic nerve head, disrupting axonal transport and RGC apoptosis [6-8]. Reduced ocular perfusion due to IOP elevation further exacerbates ischemic damage [9].

However, glaucoma can also occur with normal IOP, known as normal-tension glaucoma (NTG), where vascular dysregulation, impaired ocular blood flow autoregulation, and systemic conditions such as hypotension contribute to RGC ischemia [10-12]. Underlying mechanisms include excitotoxicity, oxidative stress, mitochondrial dysfunction and neuroinflammation, which perpetuate optic nerve degeneration [13-16]. Genetic factors further influence IOP regulation and optic nerve vulnerability, modulating individual glaucoma risk [17, 18].

The pathophysiology of glaucoma is complex and not yet fully understood and the RGC degeneration is not reversible, posing significant challenges to the development of effective treatments and limiting therapeutic outcomes.

3.1.3 Limitations of Current Treatments

Currently, the main goal of glaucoma treatment is to reduce IOP, as elevated IOP is a major risk factor for the disease [19, 20]. Treatment strategies include medications, laser treatments, and surgical interventions [21-23]. Despite their effectiveness in lowering IOP, these

approaches fail to prevent disease progression in all patients, particularly in cases of NTG, where IOP remains within normal limits [20, 24]. Moreover, even with adequate IOP control in elevated IOP glaucoma patients, some of them continue to experience progressive structural and functional damage to the optic nerve, suggesting the involvement of additional pathogenic mechanisms that are not yet fully understood [15, 25]. These challenges underscore the urgent need to develop therapeutic strategies that extend beyond IOP reduction, focusing on the neurodegenerative processes underlying glaucoma and exploring interventions that promote axonal regeneration.

3.2 Current Research on Pathways in Axonal Regeneration

The retina is an integral part of the central nervous system (CNS) and exhibits significant structural and functional similarities to the brain [26, 27]. Notably, both retinal and CNS neurons lack the ability to regenerate axons following injury [26, 27]. To address the regeneration limitation, advanced research has identified important molecular pathways that promote axonal regeneration, encompassing both intrinsic factors within neurons and extrinsic factors in the surrounding axonal microenvironment [28, 29]. Intrinsic factors include genetic and epigenetic regulators, signaling cascades, and transcriptional regulators that activate the neuronal growth program [28, 30, 31]. Extrinsic factors involve elements of the extracellular matrix, neurotrophic support, and interactions with immune and glial cells [29, 32, 33].

3.2.1 Intrinsic Pathways

Key transcriptional regulators, including KLF7, SOX11, c-Jun, and STAT3 drive the expression of growth-associated proteins essential for axonal elongation [28, 34-37]. The mTOR signaling pathway plays a central role in axonal regrowth by integrating growth-promoting cues and enhancing protein synthesis, essential for axonal repair [38, 39]. Similarly, the PI3K-Akt and MAPK/ERK pathways have emerged as critical mediators in promoting neuronal survival and axonal growth [40, 41].

Epigenetic modifications further amplify intrinsic regenerative capacity by altering chromatin structure to facilitate gene expression [30, 42]. For instance, increased histone acetylation through histone acetyltransferases like CBP/p300 enhances the transcription of genes involved in regeneration [31, 43]. Small molecules that modulate DNA methylation or histone deacetylase activity have shown promise in promoting axonal growth by reprogramming neuronal plasticity [44, 45].

3.2.2 Extrinsic Pathways

Neurotrophic factors, including BDNF, GDNF, CNTF, and NGF, are central to extrinsic support [29, 32], acting through receptors such as Trk and p75NTR to activate intracellular signaling cascades that enhance survival and promote growth [46, 47]. Innovative delivery systems, such as viral vectors and biomaterials, have been developed to sustain the localized release of these factors, improving their therapeutic potential [48, 49].

The immune system also contributes significantly to the regenerative process [50]. Macrophages play a dual role, with pro-regenerative M2-like macrophages promoting repair by secreting growth factors and cytokines such as IL-10 and IL-6 [51, 52]. Strategies to polarize macrophages toward a regenerative phenotype have shown potential in preclinical studies [51,

53]. In parallel, the modulation of glial cells, particularly astrocytes and Schwann cells, is being explored as a means to create a more permissive environment for axonal regrowth [33, 54].

3.2.3 Limitations of Recent Research on RGC Axonal Regeneration

Regeneration of RGCs involves complex crosstalk between pathways [55]. However, recent studies focus on single pathways or interventions, which overlook how intrinsic and extrinsic mechanisms interact or how systemic factors like inflammation influence both [39, 51]. This necessitates a comprehensive understanding of the molecular networks involved, for which proteomics offers unparalleled advantages [56, 57].

In adult mice, RGCs are incapable of regeneration following injury [58]. However, RGCs in neonatal mice and adult mice with lens injury retain regenerative potential [58, 59]. Therefore, identifying the physiological changes in these two regenerative animal models compared to normal adult mice—particularly those related to the activation of regenerative processes or the downregulation of regeneration-inhibitory factors—could provide critical insights into the development of therapeutic strategies for RGC regeneration.

3.3 Proteomics

3.3.1 Overview of Proteomics

Proteomics, the large-scale study of proteins, lies at the heart of modern biological research [56, 57]. Proteins serve as the functional units of life, performing roles ranging from enzymatic catalysis and structural support to signaling and regulation [56, 60]. Unlike the genome, which remains largely static, the proteome is highly dynamic, reflecting the state of a cell, tissue, or organism under specific conditions [60]. Understanding the proteome provides insight into the molecular mechanisms underpinning biological processes, diseases, and responses to therapeutic interventions.

Advances in proteomics have transformed our ability to explore this complexity. Early methods, such as two-dimensional gel electrophoresis, were pivotal in mapping protein profiles but were limited in sensitivity, reproducibility, and throughput [61]. The advent of mass spectrometry (MS)-based proteomics has revolutionized the field, enabling the identification and quantification of thousands of proteins from complex mixtures with unprecedented precision [57, 62].

3.3.2 Data-Independent Acquisition Mass Spectrometry (DIA-MS)

MS has become the cornerstone of proteomics, offering excellent sensitivity and specificity [60, 62]. Different strategies in MS-based proteomics have been developed to balance depth of coverage, quantification accuracy, and reproducibility. Among these, Data-Dependent Acquisition (DDA) and Data-Independent Acquisition (DIA) have gained significant attention [63].

DDA is a widely used approach in which the instrument selects and fragments the most abundant ions for sequencing [64, 65]. However, this strategy suffers from inherent biases, as low-abundance peptides or those in complex backgrounds are often missed [64]. In contrast, DIA-MS has emerged as a transformative technology, overcoming these limitations by systematically acquiring data from all peptides within predefined m/z windows, ensuring comprehensive and unbiased coverage [66, 67].

DIA-MS has been widely applied in various fields of biological research due to its depth and consistency. It is particularly valuable for identifying disease biomarkers, including those for cancer, cardiovascular conditions, and neurodegenerative disorders [68, 69]. Additionally, DIA-MS facilitates the study of dynamic proteomic changes in response to biological stimuli or disease progression [70, 71]. When integrated with genomic and transcriptomic data, DIA-MS enables researchers to build comprehensive models of biological systems, providing deeper

insights into molecular mechanisms [72, 73]. DIA-MS thus bridges the gap between the complexity of biological samples and the precision required for meaningful scientific insights.

3.4 Aim of the work

The aim of this study is to provide the first comprehensive proteomic map in regenerative and degenerative mouse retinas. By illustrating key proteins and pathways that are dysregulated during degeneration and activated during regeneration processes, we contribute to the development of strategies that could promote RGC survival and axon regeneration. This work not only advances the field of retinal proteomics but also paves the way for future treatments that could slow or reverse the progression of vision loss in glaucoma patients.



OPEN

Comparative proteomic analysis of regenerative mechanisms in mouse retina to identify markers for neuro-regeneration in glaucoma

Xiaosha Wang¹, Layla Fröhn¹, Panpan Li¹, Xin Shi¹, Nini Wang², Yuan Feng¹, Julia Prinz³, Hanhan Liu¹ & Verena Prokosch^{1✉}

The retina is part of the central nervous system (CNS). Neurons in the CNS and retinal ganglion cells lack the ability to regenerate axons spontaneously after injury. The intrinsic axonal growth regulators, their interaction and roles that enable or inhibit axon growth are still largely unknown. This study endeavored to characterize the molecular characteristics under neurodegenerative and regenerative conditions. Data-Independent Acquisition Mass Spectrometry was used to map the comprehensive proteome of the regenerative retina from 14-day-old mice (Reg-P14) and adult mice after lens injury (Reg-LI) both showing regrowing axons in vitro, untreated adult mice, and retina from adult mice subjected to two weeks of elevated intraocular pressure showing degeneration. A total of 5750 proteins were identified (false discovery rate < 1%). Proteins identified in both Reg-P14 and Reg-LI groups were correlated to thyroid hormone, Notch, Wnt, and VEGF signaling pathways. Common interactors comprising E1A binding protein P300 (EP300), CREB binding protein (CBP), calcium/calmodulin dependent protein kinase II alpha (CaMKII α) and sirtuin 1 (SIRT1) were found in both Reg-P14 and Reg-LI retinas. Proteins identified in both regenerating and degenerative groups were correlated to thyroid hormone, Notch, mRNA surveillance and measles signaling pathways, along with PD-L1 expression and the PD-1 checkpoint pathway. Common interactors across regenerative and degenerative retinas comprising NF-kappa-B p65 subunit (RELA), RNA-binding protein with serine-rich domain 1 (RNPS1), EP300 and SIN3 transcription regulator family member A (SIN3A). The findings from our study provide the first mapping of regenerative mechanisms across postnatal, mature and degenerative mouse retinas, revealing potential biomarkers that could facilitate neuro-regeneration in glaucoma.

Keywords RGC regeneration, Glaucoma, RGC degeneration, Mass spectrometry, Proteomic landscape

The retina constitutes a part of the central nervous system (CNS) and shares remarkable similarities to the brain. Both retinal and CNS neurons lack the capacity to regenerate axons following injury. Glaucoma, a neurodegenerative disease, shows damage to retinal ganglion cells (RGC) and their axons, ultimately leading to irreversible cell death and vision loss. Whilst enhancing the survival of RGCs is a crucial initial step in the treatment, therapies should also address axonal regeneration. However, regeneration of axons in RGCs is a complex process involving neuronal and non-neuronal changes, all working at cross-purposes, activating signaling pathways, altering the expressions of genes and proteins within the neuron that enable or inhibit axonal growth^{1,2}. Despite decades of effort and resources invested in the research of neuroregeneration, scientists are still rather far from comprehensively identifying all intrinsic axonal growth regulators and their collaborative roles.

The ability of RGCs to extend their axons decreases with age and is lost early in development³. Juvenile RGCs show spontaneous regeneration under regenerative conditions in vitro. However, even adult RGCs can regrow their axons in experimental conditions, implying that they do not lose their regenerative potential completely⁴. One approach to induce regeneration both in vivo and in vitro is accomplished by lens injury (LI) and optic

¹Department of Ophthalmology, University of Cologne, Kerpener Str. 62, 50937 Cologne, Germany. ²Cologne Excellence Cluster on Cellular Stress Responses in Aging-Associated Diseases (CECAD), Faculty of Mathematics and Natural Sciences, University of Cologne, 50931 Cologne, Germany. ³Department of Ophthalmology, RWTH Aachen University, 52074 Aachen, Germany. ✉email: verena.prokosch@uk-koeln.de

nerve crush (ONC)⁵. It is known that proteins execute their functions through interactions with other proteins. Protein–protein interaction (PPI) modalities are crucial elements that facilitate intercellular communication and modulate signal transduction pathways. Ultimately, they govern the modulatory actions of both degeneration and regeneration.

Recent advancements in mass spectrometry (MS)-based proteomic techniques, coupled with bioinformatics tools, have facilitated the comprehensive mapping of protein signaling networks across various sample types. Data-independent acquisition mass spectrometry (DIA-MS) is a next-generation proteomic methodology that provides superior reproducibility and sensitivity compared to conventional MS.

This study, building upon our previous studies^{6,7}, offers the first comprehensive exploration of the global proteome landscape, unraveling molecular intricacies and signaling pathways pivotal in both degenerative and regenerative processes in rodent retinas. These insights hold translational potential for identifying novel therapeutic targets for glaucoma.

Results

EVC induced IOP elevation

Before the EVC surgery in degeneration (Deg) group, IOP levels in eyes designated for EVC were similar to those in control eyes. After the EVC, a significant increase in IOP was observed at day 1 ($p = 0.012$), day 2 ($p < 0.0001$), day 7 ($p < 0.0001$) and day 14 post-intervention ($p = 0.003$) (Fig. 1A). Animals were sacrificed two weeks post-intervention.

EVC impairs RGC survival

EVC resulted in a significant reduction in RGC density (716.2 ± 114.7 RGC/mm²) in versus their age-matched controls (1911.7 ± 534.3 RGC/mm²) (Fig. 1B and C).

P14 and LI induced axon regeneration

On day 7 after incubation in the regenerative condition, retinas extracted from both the Reg-P14 group and the Reg-LI group demonstrated axonal outgrowth (Fig. 2A). A total outgrowth of 24 neurites was counted in the Reg-P14 group and 18 neurites per 1/8th of retina in the Reg-LI group. Explants from control and Deg groups showed no outgrowth of axons (Fig. 2B).

Proteomic profile

The proteomic profile of the retina reveals the presence of 5182 proteins in the retina of the control group, 5671 proteins in the spontaneously regenerative retina from Reg-P14 group, 5631 proteins in the experimentally regenerative retina in Reg-LI group, and 5628 proteins in the degenerative retina in Deg group. The expression profiles of all detected proteins were illustrated using a cluster heatmap (Fig. 3A). When compared to the control group, the experimental groups demonstrated distinct expression patterns. Notably, the Deg and the Reg-LI group exhibited highly similar expression patterns, indicating that the molecular responses or pathological processes involved in experimental regeneration and degeneration may converge on shared mechanisms or pathways.

DEPs across P14, LI, and Deg groups versus control

Subsequent investigation of these proteins identifies several differentially expressed proteins (DEPs) between control, Reg-P14, Reg-LI and Deg groups. The evaluation is based on the normalized abundances, and proteins were considered differentially expressed if they exhibited either a \geq twofold upregulation or a ≤ 0.5 -fold down-regulation, accompanied by adjusted p value ≤ 0.05 .

In the Reg-P14 group, a total of 1961 DEPs were identified, of which 1412 proteins were up-regulated, while 549 proteins were down-regulated (Fig. 3B). The top five upregulated proteins were identified as ASB6, FABP7, CELF4, LDB1 and PPIG. FABP7 is implicated primarily in neurogenesis and cellular proliferation within the forebrain. LDB1 play a pivotal role in retinal development, underlining its significance in visual system development. Conversely, the proteins exhibiting the most significant downregulation included GBB2, K22E, K2C1, K1C10 and ATPMK. Among these, K1C10 plays a crucial role in facilitating keratinocyte migration, which is linked to scar formation, serving as a mechanical barrier to axonal growth (Supplementary Data 1).

In the context of Reg-LI versus control, 835 DEPs were detected. Out of these, 749 proteins were found to be significantly up-regulated, while 86 proteins exhibited a significant downregulation (Fig. 3C). In the LI group, the foremost upregulated proteins were identified as CELF4, TBB4B, PPIG, TTHY and WBP2. TBB4B is integral to the organization of the microtubule cytoskeleton. In contrast, the proteins that demonstrated the most pronounced downregulation included K2C1, RAP1A, COX1, K1C42 and RL37A. Among these, COX1 is implicated in a variety of neurodegenerative diseases (Supplementary Data 2).

In the Deg group, a total of 628 DEPs were found as compared to the control retina. Among these DEPs, 565 proteins were substantially more abundant, while 63 proteins were less abundant (Fig. 3D). Among these, the top five upregulated proteins were identified as TBB4B, TTHY, ESPN, CELF4 and HPCL4. ESPN is implicated in the formation of the actin filament network, playing a critical role in cellular structure and motility. HPCL4 is pivotal in signal transduction processes, mediating the transmission of molecular signals into cellular responses. Conversely, the proteins exhibiting the most significant downregulation included RAP1A, GBB2, COX5B, PTH2 and MGST3. Among these, COX5B is implicated in mitochondrial ATP synthesis coupled proton transport. PTH2 plays crucial roles in regulation of anoikis, a form of programmed cell death (Supplementary Data 3).

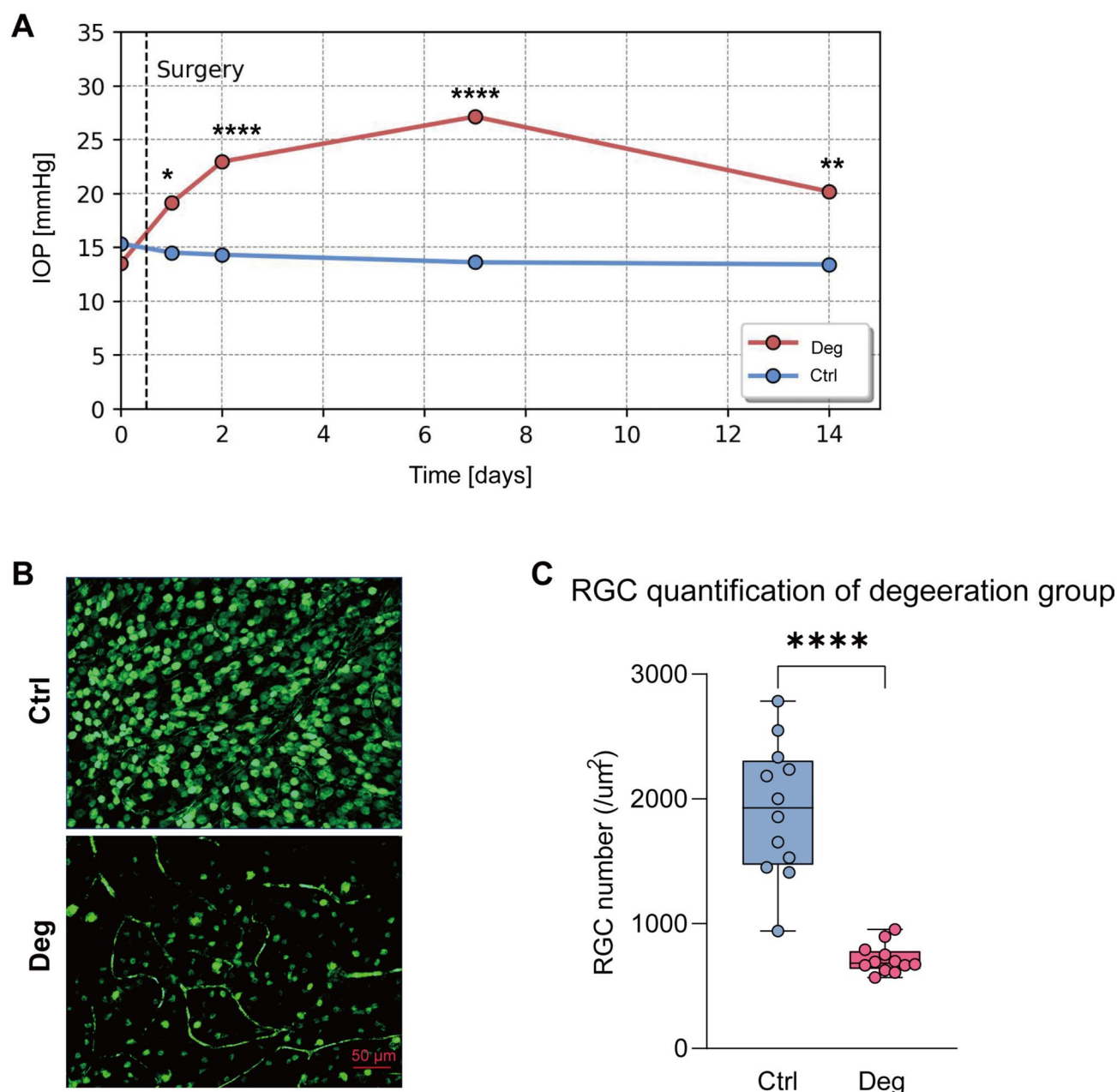


Fig. 1. Impact of Episcleral Vein Cauterization (EVC) on Intraocular Pressure (IOP) and Retinal Ganglion Cell (RGC) Density. **(A)** IOP dynamics post- EVC. **(B)** Fluorescence images of Brn3a-positive RGCs in retinal flat-mounts. **(C)** RGC density across control and EVC groups.

Pathway analysis in Reg-P14 group

KEGG pathway analysis in the Reg-P14 group identified significant enrichments in 17 pathways for proteins with increased expression and 54 pathways for those with decreased expression (Fig. 4A). Upregulated DEPs were primarily observed in genetic information processing pathways, environmental information processing pathways and organismal system were affected. The most significantly pathways from upregulated DEPs were basal transcription factors, ATP-dependent chromatin remodeling and ribosome. Downregulated DEPs predominantly impacted metabolic processes, followed by pathways implicated in human diseases and organismal systems. The most significant pathways from downregulated DEPs were metabolic pathways, oxidative phosphorylation and carbon metabolism.

Pathway analysis in Reg-LI group

KEGG pathway analysis in Reg-LI group revealed significant enrichments in eight pathways for upregulated DEPs and 3 pathways for those downregulated (Fig. 4B). Upregulated DEPs were predominantly observed in pathways related to genetic information processing. Furthermore, analysis of these upregulated DEPs revealed substantial alterations across various biological systems, including organismal systems, cellular processes, environmental

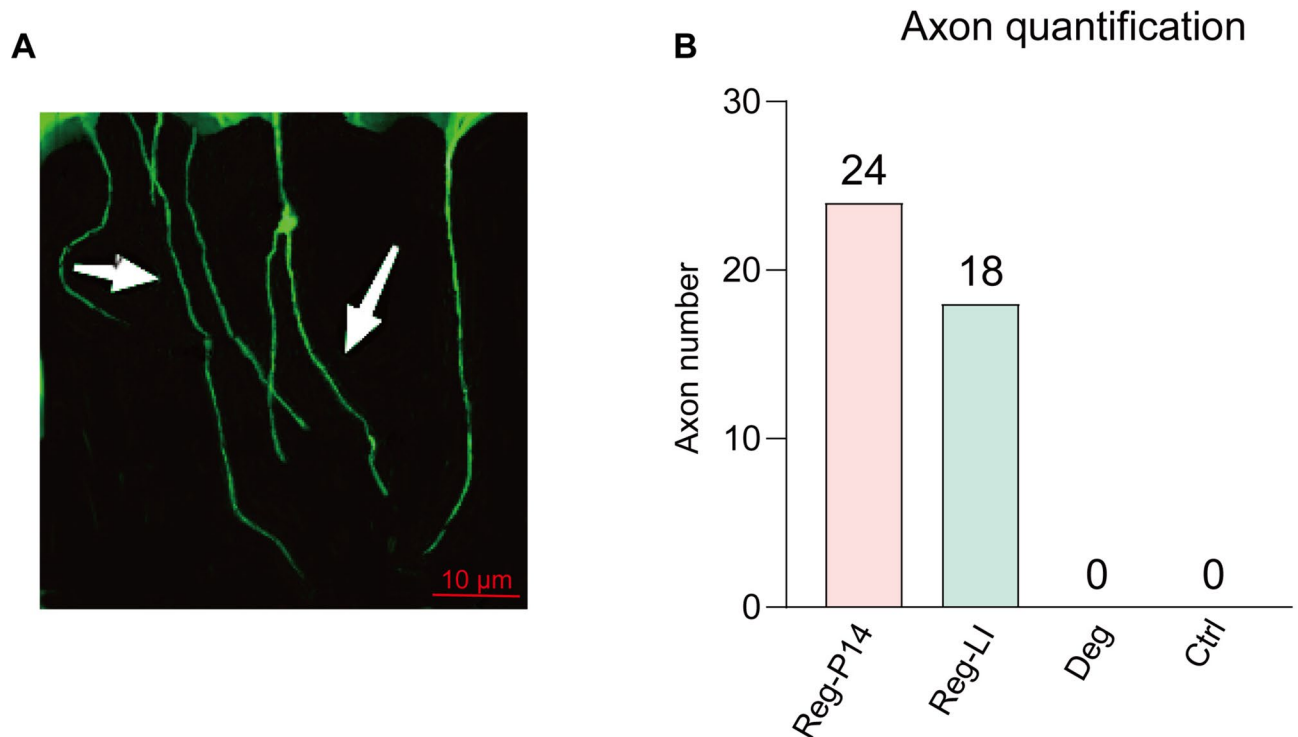


Fig. 2. Analysis of Axon Regeneration in Regenerative Postnatal Day 14 (Reg-P14), Lens Injury (Reg-LI) and degeneration (Deg) Groups. **(A)** Axonal extensions from retinal explants in the Reg- P14 group. **(B)** Evaluation and comparison of the regenerated axon numbers across Reg-P14, Reg-LI, Deg and control groups.

information processing pathways, and pathways implicated in human diseases. The most significant pathways from upregulated DEPs were thyroid hormone signaling pathway, ATP-dependent chromatin remodeling and autophagy—animal. Conversely, the most significant pathways from downregulated DEPs predominantly impacted human diseases and organismal systems. The most significant pathway from downregulated DEPs was Parkinson disease pathway.

Pathway analysis in deg group

KEGG pathway analysis in Deg group identified significant enrichments in nine pathways for upregulated DEPs and 14 pathways for downregulated DEPs (Fig. 4C). Upregulated DEPs were primarily observed in pathways associated with human diseases. Additionally, pathways related to cellular processes, organismal systems and genetic information processing were significantly affected. The most significant pathways from upregulated DEPs included measles, autophagy in animals and PD-L1 expression and the PD-1 checkpoint pathway in cancer. Conversely, pathways from downregulated DEPs predominantly impacted human diseases, followed by pathways implicated in organismal systems, metabolism and cellular processes. The most significant pathways from downregulated DEPs were chemical carcinogenesis—reactive oxygen species, diabetic cardiomyopathy and prion disease.

Comparative analysis between Reg-P14 and Reg-LI groups

Our research conducted a comprehensive comparative analysis in the Reg-p14 and Reg-LI groups. This investigation identified 708 proteins with shared regulatory patterns across both groups, identifying 1244 proteins uniquely altered in the Reg-P14 group and 125 proteins exclusively regulated in the Reg-LI group (Fig. 5A). The expression profiles of the 708 shared proteins were depicted in a cluster heatmap (Fig. 5B), showcasing expression similarities between the two groups and categorizing these proteins into 653 upregulated and 55 downregulated relative to the control group. The proteins that were most significantly upregulated include CELF4, TTHY and PPIG, while the proteins that were most significantly downregulated comprise K2C1, RAP1A and GBB2.

GO term analysis in these 708 proteins, which exhibit shared regulatory patterns across Reg-P14 and Reg-LI groups, revealed significant enrichments for 223 terms among up-regulated proteins and 4 terms among down-regulated proteins. Notably, there were 150 up-regulated proteins significantly enriched in a cluster including terms such as nervous system development, cell projection organization, neurogenesis and neuron differentiation (Supplementary Data 4). For a more comprehensive understanding of the proteins associated with neuroregeneration, a deeper functional analysis was conducted on the proteins enriched in this term cluster (Fig. 5C). The analysis highlights the biological processes, molecular functions, and cellular components central to neuroregeneration, as deduced from the examined protein set.

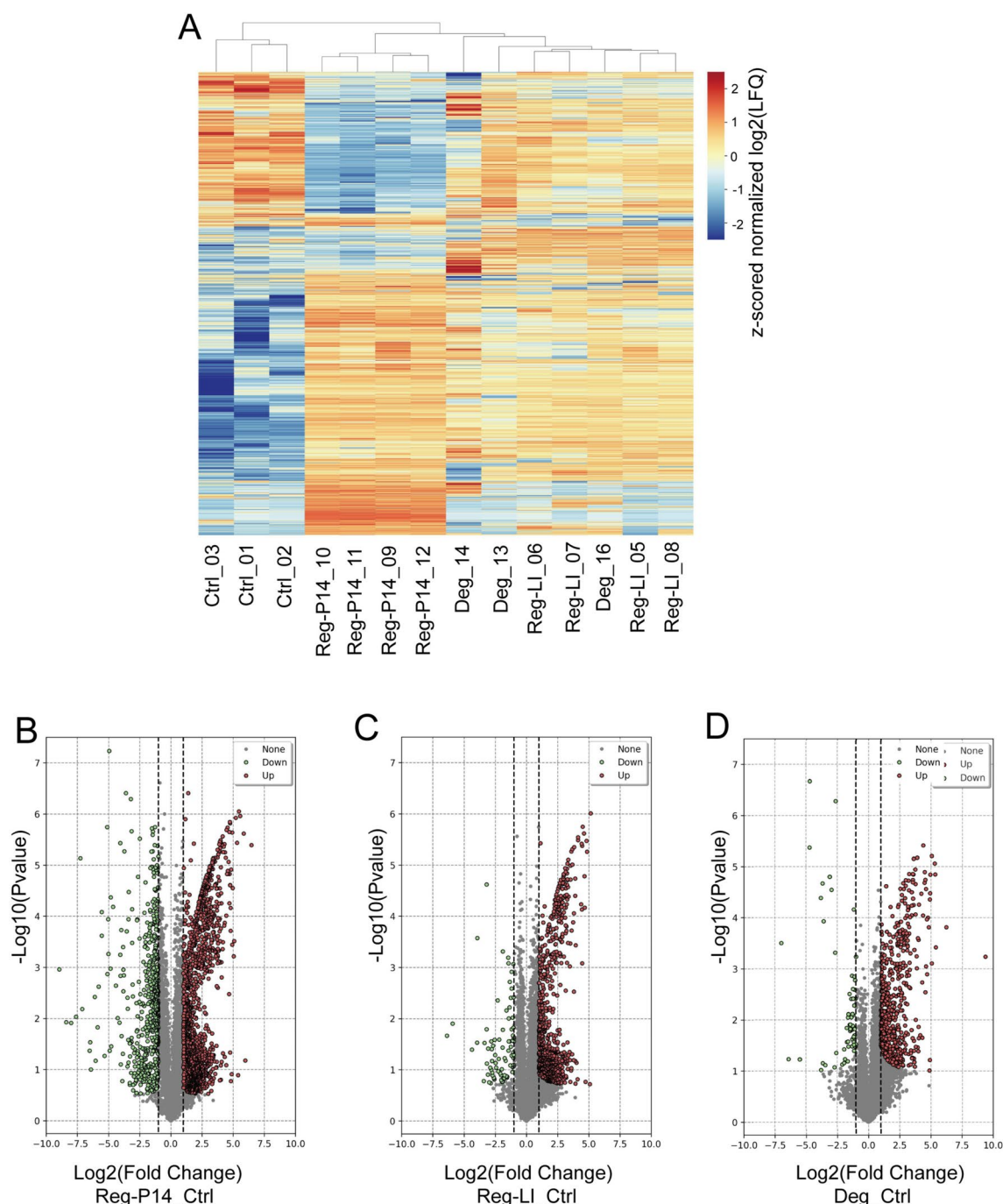


Fig. 3. Comprehensive Overview of Whole Proteomic Data. **(A)** Clustered heatmap displaying differential protein expression profiles across four experimental groups: Control (Ctrl), Postnatal Day 14 (Reg-P14), Lens Injury (Reg-LI), and Degeneration (Deg). This visualization delineates patterns of protein abundance variations among the groups. **(B–D)** Volcano plots emphasizing proteins differentially expressed in comparison to the control group across three specific conditions: **(A)** Reg-P14 versus Control; **(B)** Reg-LI versus Control; **(C)** Deg versus Control. Statistical significance was established at an adjusted p value threshold of ≤ 0.05 . Differential expression was defined by a log2 fold change greater than 1 for upregulation or less than -1 for downregulation. In these plots, red points indicate upregulated proteins and green as downregulated.

To further explore the pathways associated with the 150 neuroregeneration-related proteins enriched in the four aforementioned terms, KEGG pathway enrichment analysis was conducted. The results disclosed enrichments in 15 significant pathways, including thyroid hormone, Notch, Wnt, inositol phosphate metabolism and VEGF signaling pathways (Fig. 5D). In the integrated analysis of pathways and protein–protein interaction (PPI) networks (Fig. 5E), proteins such as SIRT1, CBP (Crebbp), EP300 and CaMKII α exhibited the most extensive

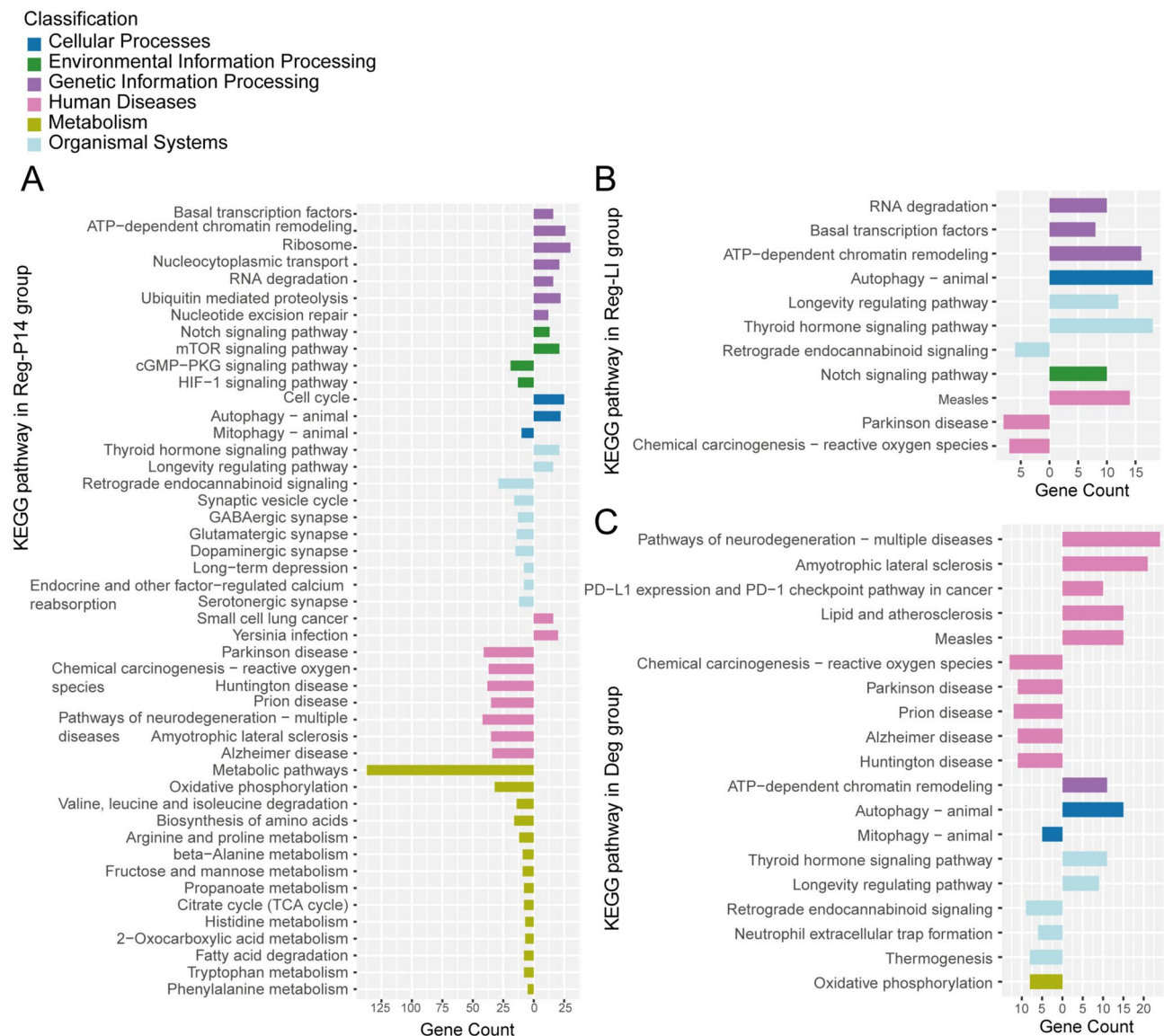


Fig. 4. KEGG Pathway Classification Map in (A) Postnatal Day 14 (Reg-P14), (B) Lens injury (Reg-LI), and (C) Degeneration (Deg) Groups. Pathways were classified into six distinct branches according to the classification system of the KEGG database. These branches include cellular processes; environmental information processing; genetic information processing; human diseases; metabolism; organismal systems. Right directions signify pathways enriched with upregulated differentially expressed proteins (DEPs), while left directions indicate pathways characterized by downregulated DEPs.

crosstalk among these pathways. Quantitative assessments of log₂ LFQ intensities reveal that these proteins are significantly upregulated in the Reg-P14 and Reg-LI experimental groups (Fig. 5F).

Comparative analysis among Reg-P14, Reg-LI and Deg groups

Our study conducted a comparative analysis among the Reg-P14, Reg-LI and Deg group. This analysis identified 410 proteins with shared regulatory patterns across all groups (Fig. 6A). The expression profiles of these shared proteins were depicted in a cluster heatmap (Fig. 6B), demonstrating expression parallels cross all groups. This heatmap sorted these shared proteins into 387 upregulated and 23 downregulated compared to the control group. The most significantly upregulated proteins included CELF4, PPIG, TTHY and WBP2 while the most downregulated were RAP1A, GBB2, MGST3 and K2C5.

The GO term analysis on 410 proteins, showing shared regulatory patterns among Reg-P14, Reg-LI and Deg groups, highlighted 102 terms linked to up-regulated proteins and 2 to down-regulated ones. Further, KEGG pathway enrichment analysis identified six significant pathways, including thyroid hormone, Notch, mRNA surveillance and measles signaling pathways, along with PD-L1 expression and the PD-1 checkpoint pathway in cancer (Fig. 6C). Integrated analysis of pathways and PPI networks (Fig. 6D) pinpointed key proteins such as

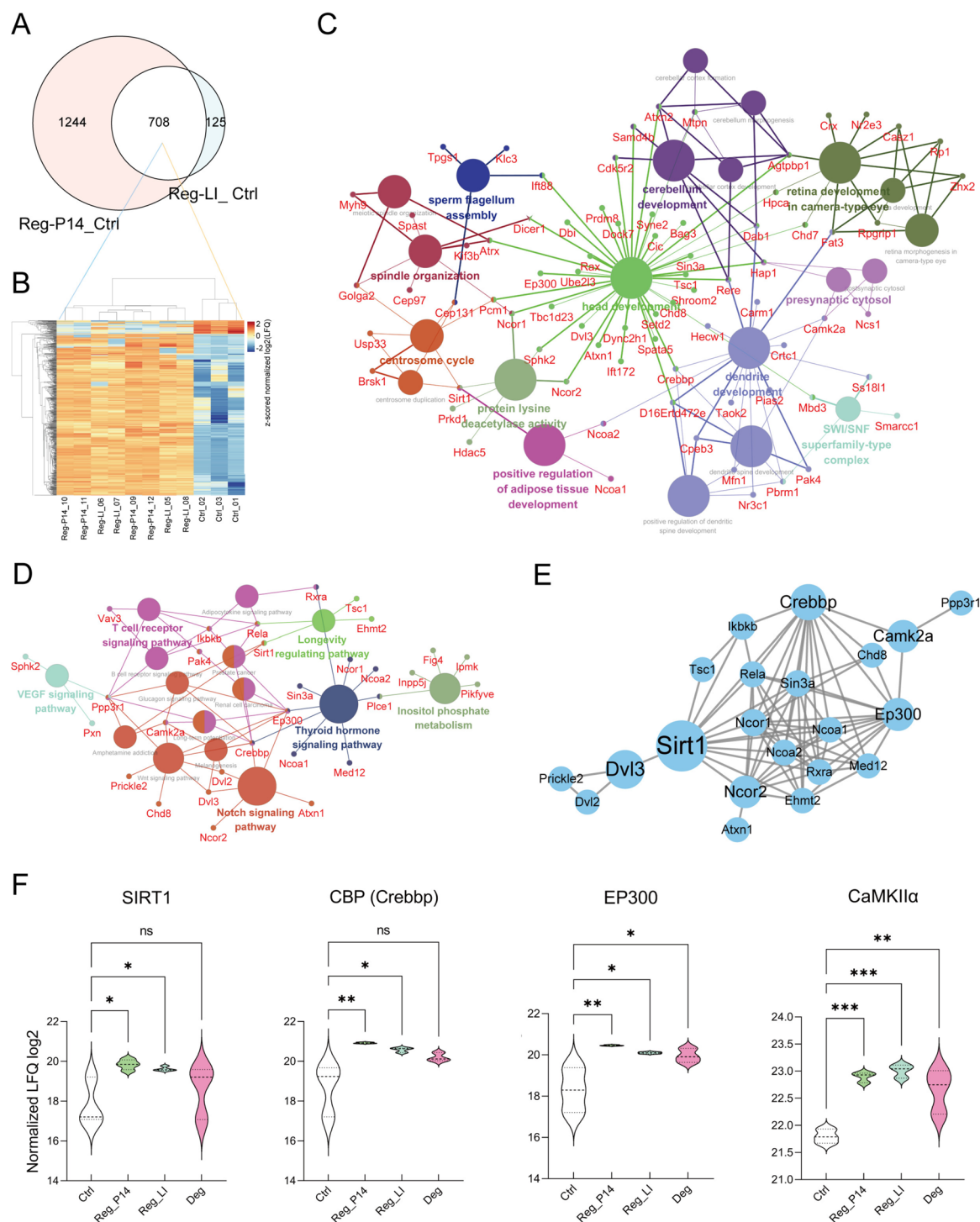


Fig. 5. Comparative Analysis between Reg-P14 and Lens Injury (Reg-LI) Groups. **(A)** A Venn diagram illustrating the overlapping and distinct DEPs between the Reg-P14 and Reg-LI groups. **(B)** A cluster map depicting the expression profiles of the 708 proteins commonly regulated in both Reg-P14 and Reg-LI groups, offering a detailed view of their expression patterns. **(C)** Gene Ontology (GO) Term and **(D)** Kyoto Encyclopedia of Genes and Genomes (KEGG) Pathway Analysis from 150 Proteins Associated with Neuro-regeneration. These figures present a clustered visualization of **(C)** GO terms and **(D)** KEGG pathways specifically related to neuro-regeneration, highlighting the proteins involved. Each circle represents a distinct GO term **(C)** or KEGG pathway **(D)**, with the size of the circle reflecting the *p* value: larger circles denote lower *p* values, indicating greater statistical significance. Circles filled with the same color represent pathways that share over 50% of their proteins, highlighting significant overlap in protein function within these pathways. **(E)** Protein-Protein Interaction (PPI) network depicting proteins enriched in the pathways shown in **(D)**. Circle sizes within this network correlate with the betweenness centrality (BC) values, and larger circle sizes mark higher BC values, indicating greater importance in the protein interaction network. **(F)** Quantitative analyses of log₂ label-free quantification (LFQ) intensities across experimental groups, offering quantitative insights into protein abundance variations.

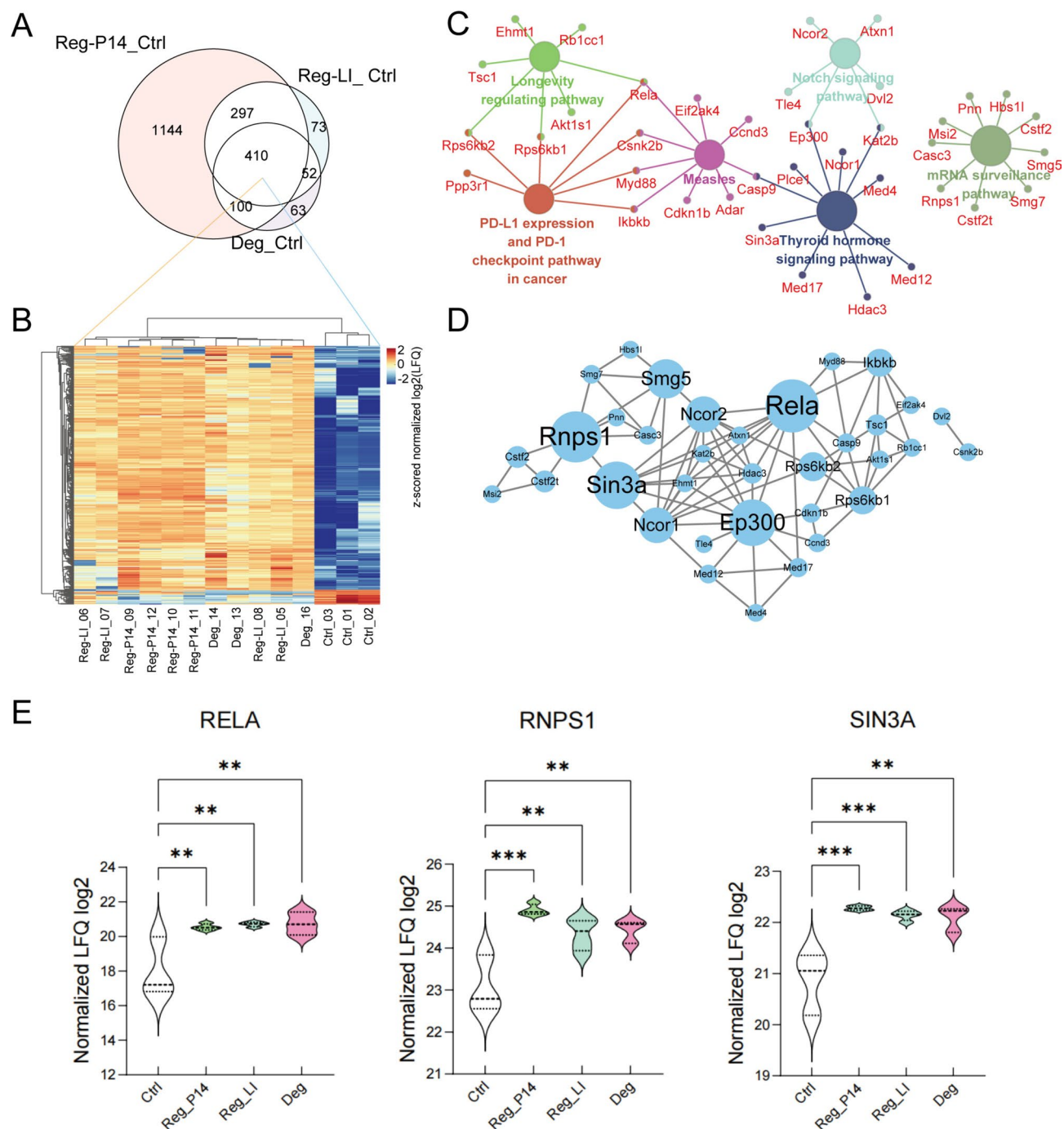


Fig. 6. Comparative Analysis among Reg-P14, Lens Injury (Reg-LI) and Degeneration (Deg) Groups. **(A)** A Venn diagram illustrating the shared and unique DEPs among Reg-P14, Reg-LI and Deg groups. **(B)** A cluster map depicting the expression profiles of the 411 proteins commonly regulated in Reg-P14, Reg-LI and Deg groups, offering a detailed view of their expression patterns. **(C)** A clustered visualization of Kyoto Encyclopedia of Genes and Genomes (KEGG) pathways from 411 proteins with shared regulatory patterns across Reg-P14, Reg-LI and Deg groups. Each circle represents a distinct KEGG pathway, with the size of the circle reflecting the *p* value: larger circles denote lower *p* values, indicating greater statistical significance. Circles filled with the same color represent pathways that share over 50% of their proteins, highlighting significant overlap in protein function within these pathways. **(D)** Protein-Protein Interaction (PPI) network depicting proteins enriched in the pathways shown in (C). Circle sizes within this network correlate with the betweenness centrality (BC) values, and larger circle sizes mark higher BC values, indicating greater importance in the protein interaction network. **(E)** Quantitative analyses of log₂ label-free quantification (LFQ) intensities across experimental groups, offering quantitative insights into protein abundance variations.

RELA, RNPS1, EP300 and SIN3A for their crucial interactions within this network. The quantification of LFQ log2 show that these proteins are significantly up-regulated in both Reg and Deg groups (Fig. 6E).

Discussion

The current study took advantage of the state-of-the-art DIA-MS technique to first, comprehensively map the whole proteome of the regenerative retina from p14 mouse pups and adult mice after LI, adult mice, and degenerative retina from adult mice subjected to 2 weeks of elevated IOP. We employed the DAVID Bioinformatics Resources and STRING database to first identify the intercellular communication and pathways lost during development, leading to the irreversible loss of intrinsic axon regeneration ability in RGCs. Additionally, we explored the putative regenerative mechanisms activated by LI. Subsequently, in an endeavor to identify potential targets that can provoke neuroregeneration in degenerative conditions, we compared the interactome and signaling pathways in the experimentally degenerative and regenerative states in the adult retina.

Proteomic characteristic in P14 mouse retina

Compared to the adult retina, the p14 sample showed significant increase in activities related to genetic information processing, cell cycle, autophagy, and specific signaling pathways like mTOR and Notch. Additionally, there was an upregulation in pathways associated with thyroid hormones and longevity. On the other hand, there was a significant decrease in metabolic activities and pathways linked to neurodegenerative diseases in the p14 sample.

Genetic Information Processing and Cell Cycle Regulation: The increase in activities related to genetic information processing and cell cycle in the p14 retina suggests a critical period of cellular proliferation and differentiation essential for retinal development. This is in line with the notion that the retina undergoes substantial growth and maturation postnatally, requiring extensive transcriptional and translational activities to produce the diverse cellular architecture characteristic of a functional retina^{8,9}.

Autophagy, mTOR, and Notch Pathways: The analysis also revealed an upregulation of autophagy and the activation of mTOR and Notch signaling pathways in the p14 retina. Autophagy plays a dual role in removing damaged cellular components, thereby maintaining cellular health, and in modulating differentiation and development¹⁰. The literature, including studies by Vazquez et al., has documented autophagy's role in neurogenesis within the olfactory bulb¹¹. The enhancement of the mTOR pathway aligns with its known functions in promoting cell growth and survival during retinal development¹². This suggests mTOR pathway may foster axon regeneration and RGC survival in the mature retina following injury, echoing the findings of Eriksen et al. on mammalian retinal regeneration¹³. Similarly, the activation of the Notch pathway, a key regulator of cell fate decisions, underscores its importance in retinal cell differentiation and the establishment of a functional retinal circuitry^{14,15}. These mechanisms collectively support a framework wherein the postnatal retina orchestrates cellular proliferation, survival, and differentiation, a requisite for both developmental processes and potential regenerative responses.

Thyroid Hormones and Longevity Pathways: The observed increase in pathways related to thyroid hormones and longevity in the p14 sample points to a regulatory role of thyroid hormones in retinal maturation and a possible enhancement of cellular defense mechanisms during this critical developmental window. This finding is consistent with the work of Arbogast et al. and Sawant et al., which suggested that thyroid hormones significantly influence retinal development and differentiation^{16,17}. Additionally, the activation of longevity pathways might indicate a stress resistance phenotype in the developing retina, potentially contributing to cell survival and function¹⁸.

Metabolic Shifts and Neurodegenerative Pathways: The observed decrease in metabolic activities could be attributed to the developmental hypoxia period, a consequence of an unestablished and dysfunctional capillary network¹⁹. This phenomenon might also suggest a potential metabolic adaptation and neuroprotective response to postnatal hypoxia²⁰. The down-regulation of neurodegenerative pathways may reflect an inherent protective mechanism against the onset of such conditions within these regenerative environments.

Regenerative mechanisms activated by LI

The comparative analysis between the p14 and LI groups revealed the reactivation of crucial signaling cascades by LI in the mature retina, with the thyroid hormone, Notch and Wnt pathways being particularly emphasized for their critical contributions to neural tissue repair and regeneration. Proteins such as CaMKIIa, CBP and EP300 exhibited the most extensive crosstalk among these pathways.

The thyroid hormone pathway is critical in regulating metabolic processes and neuroplasticity, thus enhancing neural regeneration by optimizing both the metabolic environment and transcriptional activities essential for tissue repair^{21,22}. This pathway's influence in axonal regeneration in the mature retina and nervous system aligns with findings from previous studies^{23–25}. The Notch and Wnt pathways, both intricate and evolutionarily conserved, govern a variety of cellular functions crucial for neuroregeneration^{26–28}. Particularly, the Wnt pathway plays an essential role in the proliferation and differentiation of stem cells, key processes for initiating and sustaining neural tissue regeneration²⁹. CaMKIIa, which involved in the Wnt signaling pathway, is essential for calcium signaling within neurons. It's involved in a wide range of cellular functions, including synaptic plasticity, neurotransmitter release, and gene expression³⁰. Activation of the CaMKII/CBP axis has been shown to protect long-distance RGC axon projections in vivo, maintaining visual function from the retina to the visual cortex and thus positively influencing visually guided behavior^{31,32}. CBP and EP300, implicated in all three pathways, are histone acetyltransferases vital for chromatin remodeling and gene expression regulation, facilitating the transcription of genes required for cell growth, differentiation, and repair^{33,34}. In the realm of neuroregeneration, CBP and EP300 are crucial for activating transcription of genes linked to cell survival, neuroplasticity, and axonal growth, supporting regenerative processes in both spontaneous and experimental contexts³⁵.

The integration of these pathways reveals a sophisticated regulatory network essential for activating the endogenous mechanisms of neuroregeneration. Targeting these pathways could lead to promising therapeutic strategies for enhancing neuroregeneration.

Regenerative mechanisms under degenerative conditions

The comparative analysis between the Reg-P14, Reg-LI and Deg groups depicted various pathways activated in both regenerative and degenerative conditions, notably the thyroid hormone, Notch, mRNA surveillance, and measles signaling pathways, along with PD-L1 expression and the PD-1 checkpoint pathway. Protein EP300, SIN3A, RELA and RNPS1 have been identified as pivotal interactors mediating these pathways.

The activation of the thyroid hormone and Notch signaling pathways in both spontaneously regenerative retinas from p14 mice and experimentally induced regenerative mature retinas by LI—and now observed in degenerative conditions—reaffirms the indispensable roles these pathways play in retinal regeneration under both physiological and pathological conditions. This consistency with previous findings, which documented the upregulation of these pathways in contexts of neural degeneration^{24,36}, underscores their importance in the regenerative process. EP300 is implicated in both the thyroid hormone and Notch pathways, acting as a transcriptional co-activator with a key role in chromatin remodeling and gene expression regulation³⁷. Transcriptional corepressor SIN3A, involved in thyroid hormone pathway, is responsible for the recruiting HDACs to form an HDAC-associated transcriptional complex to regulate the transcription of specific genes³⁸. It has been proved that Sin3A/HDAC is critical for mediating stage-specific neuronal gene expression and the sequential stages of neurogenesis³⁹. Their presence across different regenerative states indicates their essential function in facilitating the transcriptional responses necessary for cell proliferation, differentiation, and survival.

The mRNA surveillance pathway is crucial for maintaining the fidelity of gene expression, a fundamental process for ensuring the correct synthesis and function of proteins required during the repair and regeneration of neural tissues⁴⁰. RNPS1 (RNA-binding protein with serine-rich domain 1), which plays an important role in this pathway, mediates the increase of mRNA abundance and translational efficiency⁴¹, and provide protection from ischemic brain injury while inhibiting neuronal death⁴².

The roles of the measles signaling pathway, alongside PD-L1 expression and the PD-1 checkpoint pathway in neuroregeneration require further investigation. Their emerging significance in modulating immune system interactions with the nervous system introduces a novel aspect of neural repair mechanisms^{43,44}. Specifically, the PD-1/PD-L1 axis may play a crucial role in attenuating neuroinflammation, potentially creating a more favorable environment for neural regeneration⁴⁵. RELA (transcription factor p65), a subunit of the NF-κB complex, is implicated in both of the measles and PD-L1 pathways, mediating inflammatory responses and apoptosis⁴⁶. Reparative inflammation plays a key role in the early regenerative process with an important contribution of NF-κB signaling in initiating basal cell neurogenesis. Ablation of NF-κB signaling in regenerating neuron cells results in increased neuronal apoptosis⁴⁷. The identification of RELA in both regenerative and degenerative retina underscores its role in modulating inflammation and apoptosis during neural repair, highlighting its potential as a therapeutic target for enhancing regenerative outcomes.

In conclusion, this study depicted the complex proteomic landscape of the regenerative and degenerative retina, unveiling novel insights into the molecular drivers of retinal regeneration. Identifying key proteins and pathways, we highlight potential therapeutic targets that hold promise for revolutionizing treatments for retinal degenerative diseases. Our advancing knowledge paves the way for novel strategies to combat neurodegenerative conditions, promising a brighter future for regenerative medicine and vision restoration.

Methods
Animals

In this study, p14 C57BL/6 J mouse pups (n=4) and male C57BL/6 J mice (n=4) at the age of 8–10 weeks and a weight of 28–32 g were used. In total four types of retinal samples were used in this study. To mimic the degenerative condition in the retina, a mouse model of chronically elevated intraocular pressure (IOP), induced through the episcleral vein cauterization (EVC), was used⁴⁸. Progressive RGC degeneration was observed⁴⁹. Furthermore, two types of regenerative retinas were used: retinas from p14 mice which are spontaneously regenerative⁵⁰, and retinas from adult mice subjected to lens injury (LI), which has been proven to promote the regeneration of RGC axons in mature retinas⁵¹. Untreated retinas from adult mice served as controls. Table 1 gives an overview over the different experimental procedures.

Groups	Control	p14	LI	EVC
Animals	Male C57BL/6J mice (n=4)	p14 C57BL/6J pups (n=4)	Male C57BL/6J mice (n=4)	Male C57BL/6J mice (n=4)
Intervention	None	None	Lens injury	Elevated IOP induced by episcleral vein cauterization (EVC)
Follow-up	N/A	N/A	2 days	14 days
Cultured under regenerative conditions	7 days in culture	7 days in culture	7 days in culture	7 days in culture
Types of retinas	Non-regenerative	Spontaneously regenerative	Experimentally regenerative	Degenerative
Immunohistochemistry	Anti-Brn3a	Anti-beta-III-tubulin	Anti-beta-III-tubulin; Anti-Brn3a	Anti-Brn3a
DIA-MS	Yes	Yes	Yes	Yes

Table 1. Overview of the different groups and their outcomes.

Animal experiments were approved by the State Office for Nature, Environment and Consumer Protection North Rhine-Westphalia (LANUV Landesamt für Natur, Umwelt und Verbraucherschutz Nordrhein-Westfalen, permission number: 81-02.04.2020. A490; approval date: 25.03.2021). All experimental procedures adhered to the guidelines outlined in the Association for Research in Vision and Ophthalmology (ARVO) Statement for the Use of Animals in Ophthalmic and Vision Research, as well as the protocols established by the Institutional Animal Care and Use Committee. Our study is reported in accordance with Animal Research: Reporting of In Vivo Experiments (ARRIVE) guidelines. The animals were housed within the Animal Facilities of the Medical Faculty at the University of Cologne with a 12-h day-night cycle. Water and food were facilitated *ad libitum*.

Surgical procedures were conducted under general anesthesia, administered through intraperitoneal injection. The anesthetic protocol comprised a combination of 0.50 ml Xylazinehydrochloride (Xylazine, Dutch Farm International, Germany) and 1.00 ml Ketamine (Ketamine Inresa, Inresa Arzneimittel GmbH, Germany), diluted in 8.5 ml of sodium chloride. The dosage was calibrated at 0.1 ml per 10 g of body weight. Oxybuprocaine hydrochloride (Novesine, OmniVision, Puchheim, Germany) was applied topically to the ocular surfaces before the intervention. All animals were observed directly by the staff at the animal facilities of the medical faculty of Cologne after each surgery and once a day until euthanasia.

Lens injury (LI) to induce regeneration of RGC axons in mature retina

Adult male C57BL6J mice ($n = 4$) were anesthetized as described above. Lens injury was performed in the right eye while the left eye served as control. After administration pupil dilatation with mydriatic (Tropicamide, PZN-01875775), LI was induced by puncturing the lens capsule using a 30G needle via a retro-lenticular approach as described before⁵¹. The tip of the needle was bent at a 90° angle and inserted into the eye perpendicular to the sclera so as to intentionally puncture the lens capsule.

Episcleral vein cauterization (EVC) to induce elevated IOP

Chronically elevated IOP was induced through the cauterization of three episcleral veins in the right eyes of the adult male C57BL6J mice ($n = 4$) and the left eyes served as control, following previously established protocols⁵². In brief, following anesthesia, an incision was made on the conjunctiva and Tenon's capsule to expose the episcleral veins. The major trunks of these veins were then cauterized using an ophthalmic small vessel cauterizer (Fine Science Tools GmbH, 18000-00, Germany). Subsequently, the conjunctiva was carefully readjusted and ofloxacin ointment was given onto the ocular surface to prevent infection. To assess IOP changes, measurements were taken before and right after the surgery and at intervals at day 1, day 2, day 7 and day 14 post-surgery, using a TonoLab rebound tonometer (iCare, Vantaa, Finland) on conscious animals^{53,54}.

Preparation of retinal explants

The adult mice and the p14 pups were euthanized via cervical dislocation. Eyes were enucleated immediately post-mortem and transferred to a petri dish containing ice-cold betaisadona solution (Braunol, Braun, Germany) for 3 min and medium was then changed into ice-cold sterile Hank's Balanced Salt Solution (HBSS; Gibco BRL, Eggenstein, Germany). The anterior segment of the eye was detached and the retina uncovered. The intact retina was separated from the optic cup and the vitreous body was removed. Explants were placed with the ganglion cell layer up on Millipore filters (A045R047Z-P, Japan). The retinal explants from adult mice were carefully dissected into 4 quarters for further experiments or analysis.

Culture under regenerative conditions

Retinas from P14, LI, EVC and control groups were carefully dissected and whole-mounted on mixed cellulose filters (A045R047Z-P, Japan). Each whole-mounted retina was divided radially into four sections using a McIlwain tissue chopper. Subsequently, one quarter of the retina was further segmented radially into two parts using the same instrument, each part was cultured in a lumox culture dish 50 (94.6077.410) pre-coated with poly-D-lysine and laminin, as described in detail in our previous study⁵⁵. Serum-free S4 growth medium as described in our previous study was used⁵⁵. The retinal explants were positioned with the ganglion cell layer facing down. These explants were incubated at 37 °C in an atmosphere of 5% CO₂ and 55% O₂ for a duration of 7 days.

Quantification of RGCs

In total three retinal quarters per group were used for RGC quantification to validate neurodegeneration after EVC. RGCs in retinal explants were labeled by Brn3a immunohistochemical staining as previously described^{56,57}. Briefly, the retinal explants were washed in phosphate-buffered saline (PBS), fixed in 4% paraformaldehyde (PFA; pH = 7.4), and then in 30% sucrose solution overnight. Non-specific binding was blocked with 1% milk powder and 0.3% Triton in PBS. The tissues were subsequently incubated with primary antibody overnight at 4 °C, followed by washing, and then exposed to Alexa-Fluor-488-conjugated secondary antibody (1:1000) for 2 h in darkness. The explants were then washed and mounted using antifade mounting media with 4'6-Diamidino-2-phenylindol (DAPI, VEC-H-1200). Fluorescence-positive RGCs were visualized and photographed with a fluorescent microscope under 20-fold magnification (Imager.M2 ApoTome.2 Carl Zeiss, Germany, 4 pictures per retinal quarter). Total numbers of RGCs were counted using ImageJ (ImageJ Fiji version 1.5). An average value per retinal quarter was calculated and then converted to RGCs/mm². Mean values were compared between groups. Primary antibodies used were mouse anti-brain-specific homeobox/POU domain protein 3A (Brn-3a) monoclonal antibody (1:200; EMD Millipore Corp., MAB1585, USA). Secondary antibodies used were goat anti-mouse conjugated with Alexa Flour 488 (1:1000; abcam, ab150113).

Immunohistochemistry of RGC axons

After 7 days in culture, outgrowing neurites have been visualized and photographed natively with a binocular microscope ($n = 8$) with 40-fold magnification. On day 7 post explantation, neurites were identified immunohistologically by anti- β -III-Tubulin (Purified anti-Tubulin β 3, BioLegend). In brief the retinal explants with their neurites were fixed inside of the petri dishes in 4%-formalin-solution, blocked in 2% bovine serum albumin, 0.3% Triton-X and 5% goat serum for 60 min. The β -III-Tubulin-AB was diluted in blocking solution and incubated overnight at 4 °C. Following neurites were visualized with a fluorescent microscope (Nikon Eclipse TS100, Germany) using 20-fold magnification. Under usage of Image J neurites have been counted. Subsequently, mean values of the particular experimental groups were calculated and compared. Images were processed and presented using GNU Image Manipulation Program (GIMP 2.10.34).

Sample preparation for mass spectrometry

Retinal proteins were extracted by tissue protein extraction reagent (T-PER, Thermo Scientific, MA, USA) as described previously by Manicam et al.⁵⁸. Homogenization of the tissue was achieved using a tissue squasher. Subsequently, the sample was subjected to centrifugation at 10,000 $\times g$ for a duration of 5 min, resulting in the pelleting of tissue debris. The supernatant was then carefully collected, and the protein concentration for each sample was determined using a standard bicinchoninic acid (BCA) protein assay kit (Pierce, Rockford, IL, USA). This quantification procedure was executed in accordance with the manufacturer's instructions. Samples with a protein concentration exceeding 1 $\mu\text{g}/\mu\text{L}$ underwent further processing via SP3 sample preparation. In detail, the SP3 preparation process involved adding an equal volume of 2 \times SP3 lysis buffer, consisting of 10% SDS in PBS, to the respective samples. The resultant mixture was homogenized through pipetting and subsequently subjected to a heat treatment at 95 °C for 5 min. To facilitate reduction, 100 mM Dithiothreitol (DTT) was added to each sample, achieving a final concentration of 5 mM. Subsequent to vortexing, the samples were incubated at 55 °C for a duration of 30 min. The alkylation process involved the addition of 400 mM Chloroacetamide (CAA), reaching a final concentration of 40 mM. Following thorough vortexing, the samples were incubated in the dark at room temperature for 30 min, shielded by tin foil. Then the samples were once again subjected to centrifugation at 20,000 $\times g$ for a period of 10 min. Subsequently, the supernatant was carefully transferred to new tubes. Finally, to ensure sample preservation, they were frozen at -20 °C and subsequently submitted to the CECAD/CMMC proteomics core facility at the University of Cologne for further DIA-MS.

Mass spectrometry analysis

Samples were analyzed by the Cologne Excellence Cluster for Aging and Aging-related Diseases (CECAD Proteomics Facility, Cologne, Germany) on an Orbitrap Exploris 480 (Thermo Scientific, granted by the German Research Foundation under INST 1856/71-1 FUGG) mass spectrometer equipped with a FAIMSpro differential ion mobility device that was coupled to an UltiMate 3000 (Thermo Scientific). Samples were loaded onto a precolumn (Acclaim 5 μm PepMap 300 μ Cartridge) for 2 min at 15 μL flow before reverse-flushed onto an in-house packed analytical column (30 cm length, 75 μm inner diameter, filled with 2.7 μm Poroshell EC120 C18, Agilent). Peptides were chromatographically separated at a constant flow rate of 300 nL/min and the following gradient: initial 6% B (0.1% formic acid in 80% acetonitrile), up to 32% B in 72 min, up to 55% B within 7.0 min and up to 95% solvent B within 2.0 min, followed by column wash with 95% solvent B and reequilibration to initial condition. The FAIMS pro was operated at -50 V compensation voltage and electrode temperatures of 99.5 °C for the inner and 85 °C for the outer electrode.

For the gas-phase fractionated library, a pool generated from all samples was analyzed in six individual runs covering the range from 400 m/z to 1000 m/z in 100 m/z increments. For each run, MS1 was acquired at 60 k resolution with a maximum injection time of 98 ms and an AGC target of 100%. MS2 spectra were acquired at 30 k resolution with a maximum injection time of 60 ms. Spectra were acquired in staggered 4 m/z windows, resulting in nominal 2 m/z windows after deconvolution using ProteoWizard⁵⁹.

For the samples, MS1 scans were acquired from 399 to 1001 m/z at 15 k resolution. Maximum injection time was set to 22 ms and the AGC target to 100%. MS2 scans ranged from 400 to 1000 m/z and were acquired at 15 k resolution with a maximum injection time of 22 ms and an AGC target of 100%. DIA scans covering the precursor range from 400 to 1000 m/z and were acquired in 60 \times 10 m/z windows with an overlap of 1 m/z . All scans were stored as centroid.

The gas-phase fractionated library was built using DIA-NN 1.8.1@⁶⁰ using A Swissprot mouse canonical database (UP589, downloaded 04/01/22) with settings matching acquisition parameters. Samples were analyzed in DIA-NN 1.8.1 as well using the previously generated library and identical database. DIA-NN was run with the additional command line prompts “—report-lib-info” and “—relaxed-prot-inf”. Further output settings were: filtered at 0.01 FDR, N-terminal methionine excision enabled, maximum number of missed cleavages set to 1, min peptide length set to 7, max peptide length set to 30, min precursor m/z set to 400, max precursor m/z set to 1000, cysteine carbamidomethylation enabled as a fixed modification. Afterwards, DIA-NN output was further filtered on library q -value and global q -value ≤ 0.01 and at least two unique peptides per protein using R (4.1.3). Finally, label-free quantification (LFQ) values calculated using the DIA-NN R-package. Afterwards, analysis of results was performed in Perseus 1.6.15@⁶¹. Normalized LFQ data from DIA-NN for proteins with at least two unique peptides were log2 transformed and samples checked for data quality based on identified proteins and two samples were removed due to low protein identifications. Afterwards, proteins IDs were filtered for data completeness removing all proteins not present in all samples of at least one replicate group and remaining proteins annotated for GO, KEGG, Pfam and Reactome pathway names. Imputation was performed using the MinDet algorithm from the ImputeLCMD package embedded into the Perseus R plugin⁶². Finally, one-way ANOVA and T-tests (Student's or Welch's, depending on even or uneven replicate numbers in specific comparison) were

performed to identify significantly changed proteins. All tests were FDR-based with a cutoff of 0.05 and s_0 of 0.2. All detected proteins were Z-scored and used for hierarchical clustering with standard conditions.

Enrichment analysis

The identification and visualization of differentially expressed proteins (DEPs) were executed using Python code. Significance was determined based on a cutoff value of FDR adjusted p value ≤ 0.05 , and differential expression was defined as a log2 Fold change > 1 or < -1 . Gene Ontology (GO) term and Kyoto Encyclopedia of Genes and Genomes (KEGG) pathway enrichment analyses were conducted employing DAVID Bioinformatics Resources (<https://david.ncifcrf.gov/tools.jsp>)^{63,64} and KEGG database (<https://www.kegg.jp>)^{65–67}. Statistical significance was defined as FDR < 0.05 . Protein–protein interactions were undertaken with the String database (<https://string-db.org/>). ClueGO and CytoNCA plugins within Cytoscape were employed for the graphical representation of enrichment outcomes.

Statistical analysis

Statistical analyses for RGC quantification and IOP, along with figure presentation, were conducted using Prism 8 software (GraphPad Software, Inc., San Diego, CA, USA). The data are presented as mean \pm standard deviation (SD). The assessment of significant differences between groups was performed using either a one-way analysis of variance (ANOVA) or an unpaired t -test. Statistical significance was defined as $p < 0.05$.

The overview of experimental procedures encompassing animal modeling, sample preparation, and the proteomics workflow employed in this investigation, is presented in Fig. 7.

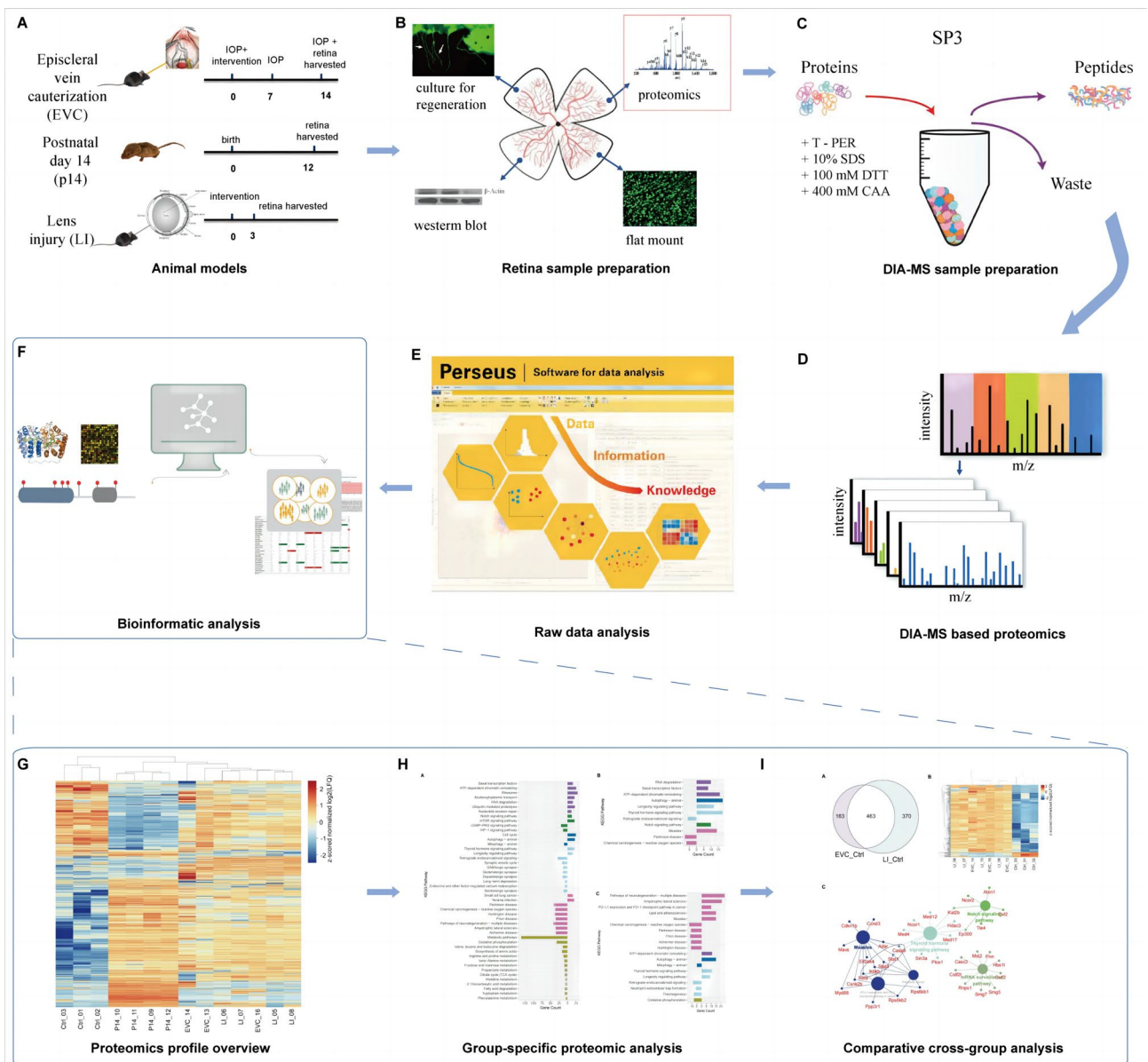


Fig. 7. Experimental Workflow Overview. **(A)** Animal model establishment: Glaucomatous retinal ganglion cell (RGC) degeneration models were induced in 9-week-old C57BL/6J mice through episcleral vein cauterization (EVC). Experimental RGC regeneration was initiated by lens injury (LI) in 9-week-old C57BL/6J mice. Mice were euthanized at specific time points: 2 weeks post-EVC surgeries, 14 days post-birth (p14), and 2 days after LI. **(B)** Retina harvesting and preparation: After successful animal model establishment, retinas were harvested and prepared for diverse analytical techniques, including proteomic analysis, regeneration culture, and immunohistochemistry (IHC). **(C)** DIA-MS sample preparation (SP3 Protocol): Retinal samples underwent preparation for DIA-MS using the Single-Pot Solid-Phase-enhanced Sample Preparation (SP3) protocol. **(D,E)** DIA-MS-based proteomic analysis: Prepared samples underwent comprehensive DIA-MS-based proteomic analysis to profile the retinal proteome, allowing quantitative assessment of protein abundance and expression. **(F)** Bioinformatic analysis: The acquired proteomic data underwent bioinformatic analyses: **(G)** Proteomics profile overview: This panel presents a comprehensive overview of the proteomic datasets employed for subsequent analytical processes. **(H)** Group-specific proteomic analysis: This section illustrates detailed pathway analyses for the p14, LI, and EVC groups, elucidating the distinct proteomic signatures associated with each experimental condition. **(I)** Comparative cross-group analysis: This analysis compares proteomic profiles across different experimental groups, aiming to pinpoint both unique and shared molecular expressions, pathways, and interactions.

Data availability

The data that support the findings of this study have been deposited in ProteomeXchange with identifier PXD049992. https://www.ebi.ac.uk/pride/profile/reviewer_pxd049992 (Reviewer account details: Username: reviewer_pxd049992@ebi.ac.uk, Password: fou5SAeC).

Received: 23 May 2024; Accepted: 6 September 2024

Published online: 04 October 2024

References

- Prokosch, V. *et al.* Deciphering proteins and their functions in the regenerating retina. *Expert Rev. Proteomics* **7**(5), 775–795 (2010).
- Eastlake, K. *et al.* Comparison of proteomic profiles in the zebrafish retina during experimental degeneration and regeneration. *Sci. Rep.* **7**, 44601 (2017).
- Goldberg, J. L. *et al.* Amacrine-signaled loss of intrinsic axon growth ability by retinal ganglion cells. *Science* **296**(5574), 1860–1864 (2002).
- Bohm, M. R. *et al.* betaB2-crystallin promotes axonal regeneration in the injured optic nerve in adult rats. *Cell Transplant.* **24**(9), 1829–1844 (2015).
- Fischer, D., Heiduschka, P. & Thanos, S. Lens-injury-stimulated axonal regeneration throughout the optic pathway of adult rats. *Exp. Neurol.* **172**(2), 257–272 (2001).
- Liu, H. *et al.* Proteomics reveals the potential protective mechanism of hydrogen sulfide on retinal ganglion cells in an ischemia/reperfusion injury animal model. *Pharmaceuticals (Basel)* **13**(9), 213 (2020).
- Anders, F. *et al.* Proteomic profiling reveals crucial retinal protein alterations in the early phase of an experimental glaucoma model. *Graefes Arch. Clin. Exp. Ophthalmol.* **255**(7), 1395–1407 (2017).
- Suzuki, F. *et al.* Overexpression of neural miRNAs miR-9/9* and miR-124 suppresses differentiation to Muller glia and promotes differentiation to neurons in mouse retina in vivo. *Genes Cells* **25**(11), 741–752 (2020).
- Zhang, S. S. *et al.* A biphasic pattern of gene expression during mouse retina development. *BMC Dev. Biol.* **6**, 48 (2006).
- Baehrecke, E. H. Autophagy: Dual roles in life and death?. *Nat. Rev. Mol. Cell Biol.* **6**(6), 505–510 (2005).
- Vazquez, P. *et al.* Atg5 and Ambra1 differentially modulate neurogenesis in neural stem cells. *Autophagy* **8**(2), 187–199 (2012).
- Zelinka, C. P. *et al.* mTor signaling is required for the formation of proliferating Muller glia-derived progenitor cells in the chick retina. *Development* **143**(11), 1859–1873 (2016).
- Eriksen, A. Z. *et al.* Multifarious biologic loaded liposomes that stimulate the mammalian target of rapamycin signaling pathway show retina neuroprotection after retina damage. *ACS Nano* **12**(8), 7497–7508 (2018).
- Shi, S. Y., Pei, C. W. & Chen, X. L. Role of Notch signaling pathway in retina development and angiogenesis. *Zhonghua Yan Ke Za Zhi* **47**(12), 1147–1150 (2011).
- Taylor, S. M. *et al.* The bHLH transcription factor NeuroD governs photoreceptor genesis and regeneration through delta-notch signaling. *Invest. Ophthalmol. Vis. Sci* **56**(12), 7496–7515 (2015).
- Arbogast, P. *et al.* Thyroid hormone signaling in the mouse retina. *PLoS ONE* **11**(12), e0168003 (2016).
- Sawant, O. *et al.* Light-regulated thyroid hormone signaling is required for rod photoreceptor development in the mouse retina. *Invest. Ophthalmol. Vis. Sci.* **56**(13), 8248–8257 (2015).
- Ashraf, H. J. *et al.* Comparative transcriptome analysis of (Hymenoptera: Eulophidae) reveals differentially expressed genes upon heat shock. *Comp. Biochem. Physiol. D Genomics Proteomics* **41**, 100940 (2022).
- Grimm, C. & Willmann, G. Hypoxia in the eye: A two-sided coin. *High Alt. Med. Biol.* **13**(3), 169–175 (2012).
- Arduini, A. *et al.* Metabolic adaptation and neuroprotection differ in the retina and choroid in a piglet model of acute postnatal hypoxia. *Pediatr Res.* **76**(2), 127–134 (2014).
- Mullur, R., Liu, Y. Y. & Brent, G. A. Thyroid hormone regulation of metabolism. *Physiol. Rev.* **94**(2), 355–382 (2014).
- Desouza, L. A. *et al.* Thyroid hormone regulates the expression of the sonic hedgehog signaling pathway in the embryonic and adult Mammalian brain. *Endocrinology* **152**(5), 1989–2000 (2011).
- Bhumika, S. & Darras, V. M. Role of thyroid hormones in different aspects of nervous system regeneration in vertebrates. *Gen. Comp. Endocrinol.* **203**, 86–94 (2014).
- Sohn, E. J. & Park, H. T. Differential expression of circular RNAs in the proximal and distal segments of the sciatic nerve after injury. *Neuroreport* **31**(1), 76–84 (2020).
- Zhang, X. *et al.* The potential role of eyestalk in the immunity of to infection II. From the perspective of long non-coding RNA. *Fish Shellfish Immunol.* **124**, 300–312 (2022).
- Moldovan, G. E., Miele, L. & Fazleabas, A. T. Notch signaling in reproduction. *Trends Endocrinol. Metab.* **32**(12), 1044–1057 (2021).
- Campbell, L. J. *et al.* Retinal regeneration requires dynamic Notch signaling. *Neural. Regen. Res.* **17**(6), 1199–1209 (2022).
- Waqas, M. *et al.* Role of Wnt and Notch signaling in regulating hair cell regeneration in the cochlea. *Front. Med.* **10**(3), 237–249 (2016).
- Duan, R. S. *et al.* Wnt3 and Gata4 regulate axon regeneration in adult mouse DRG neurons. *Biochem. Biophys. Res. Commun.* **499**(2), 246–252 (2018).
- Hell, J. W. CaMKII: Claiming center stage in postsynaptic function and organization. *Neuron* **81**(2), 249–265 (2014).
- Guo, X. *et al.* Preservation of vision after CaMKII-mediated protection of retinal ganglion cells. *Cell* **184**(16), 4299–4314 e12 (2021).
- Yan, X. D. *et al.* CaMKII-mediated CREB phosphorylation is involved in Ca-induced BDNF mRNA transcription and neurite outgrowth promoted by electrical stimulation. *Plos ONE* **11**(9), 55 (2016).
- Nicosia, L. *et al.* Therapeutic targeting of EP300/CBP by bromodomain inhibition in hematologic malignancies. *Cancer Cell* **41**(12), 2136–2153 e13 (2023).
- Anderson, J., Bhandari, R. & Kumar, J. P. A genetic screen identifies putative targets and binding partners of CREB-binding protein in the developing Drosophila eye. *Genetics* **171**(4), 1655–1672 (2005).
- Hutson, T. H. *et al.* Cbp-dependent histone acetylation mediates axon regeneration induced by environmental enrichment in rodent spinal cord injury models. *Sci. Transl. Med.* <https://doi.org/10.1126/scitranslmed.aaw2064> (2019).
- Wei, C. *et al.* Expression of Notch and Wnt/beta-catenin signaling pathway in acute phase severe brain injury rats and the effect of exogenous thyroxine on those pathways. *Eur. J. Trauma Emerg. Surg.* **47**(6), 2001–2015 (2021).
- Ghosh, A. K. p300 in cardiac development and accelerated cardiac aging. *Aging Dis.* **11**(4), 916–926 (2020).
- Saunders, A. *et al.* The SIN3A/HDAC corepressor complex functionally cooperates with NANOG to promote pluripotency. *Cell Rep.* **18**(7), 1713–1726 (2017).
- Zhang, B. *et al.* Transcriptome analysis of Schwann cells at various stages of myelination implicates chromatin regulator Sin3A in control of myelination identity. *Neurosci. Bull.* <https://doi.org/10.1007/s12264-022-00850-9> (2022).
- Popp, M. W. & Maquat, L. E. Organizing principles of mammalian nonsense-mediated mRNA decay. *Annu. Rev. Genet.* **47**, 139–165 (2013).
- Mabin, J. W. *et al.* The exon junction complex undergoes a compositional switch that alters mRNP structure and nonsense-mediated mRNA decay activity. *Cell Rep.* **25**(9), 2431 (2018).

42. Zhang, Z. *et al.* RNPS1 inhibition aggravates ischemic brain injury and promotes neuronal death. *Biochem. Biophys. Res. Commun.* **523**(1), 39–45 (2020).
43. Dhib-Jalbut, S. *et al.* Failure of measles virus to activate nuclear factor-kappa B in neuronal cells: Implications on the immune response to viral infections in the central nervous system. *J. Immunol.* **162**(7), 4024–4029 (1999).
44. Zhao, J. *et al.* PD-L1/PD-1 checkpoint pathway regulates hippocampal neuronal excitability and learning and memory behavior. *Neuron* **111**(17), 2709–2726 e9 (2023).
45. Chauhan, P. & Lokensgard, J. R. Glial cell expression of PD-L1. *Int. J. Mol. Sci.* **20**(7), 1677 (2019).
46. Viatour, P. *et al.* Phosphorylation of NF-kappaB and IkappaB proteins: Implications in cancer and inflammation. *Trends Biochem. Sci.* **30**(1), 43–52 (2005).
47. Chen, M., Reed, R. R. & Lane, A. P. Acute inflammation regulates neuroregeneration through the NF-kappaB pathway in olfactory epithelium. *Proc. Natl. Acad. Sci. U.S.A.* **114**(30), 8089–8094 (2017).
48. Ruiz-Ederra, J. & Verkman, A. S. Mouse model of sustained elevation in intraocular pressure produced by episcleral vein occlusion. *Exp. Eye Res.* **82**(5), 879–884 (2006).
49. Wang, M. *et al.* Intraocular pressure-induced endothelial dysfunction of retinal blood vessels is persistent, but does not trigger retinal ganglion cell loss. *Antioxidants (Basel)* **11**(10), 1864 (2022).
50. Hirsch, S. & Bahr, M. Immunocytochemical characterization of reactive optic nerve astrocytes and meningeal cells. *Glia* **26**(1), 36–46 (1999).
51. Fischer, D., Pavlidis, M. & Thanos, S. Cataractogenic lens injury prevents traumatic ganglion cell death and promotes axonal regeneration both in vivo and in culture. *Invest. Ophthalmol. Vis. Sci.* **41**(12), 3943–3954 (2000).
52. Gericke, A. *et al.* Elevated intraocular pressure causes abnormal reactivity of mouse retinal arterioles. *Oxid. Med. Cell. Longev.* **2019**, 9736047 (2019).
53. Chen, H. *et al.* Progressive degeneration of retinal and superior collicular functions in mice with sustained ocular hypertension. *Invest. Ophthalmol. Vis. Sci.* **56**(3), 1971–1984 (2015).
54. Thomson, B. R. *et al.* Angiopoietin-1 knockout mice as a genetic model of open-angle glaucoma. *Transl. Vis. Sci. Technol.* **9**(4), 16 (2020).
55. Bahr, M., Vanselow, J. & Thanos, S. In vitro regeneration of adult rat ganglion cell axons from retinal explants. *Exp. Brain Res.* **73**(2), 393–401 (1988).
56. Nadal-Nicolas, F. M. *et al.* Long-term effect of optic nerve axotomy on the retinal ganglion cell layer. *Invest. Ophthalmol. Vis. Sci.* **56**(10), 6095–6112 (2015).
57. Nadal-Nicolas, F. M. *et al.* Displaced retinal ganglion cells in albino and pigmented rats. *Front. Neuroanat.* **8**, 99 (2014).
58. Manicam, C. *et al.* First insight into the proteome landscape of the porcine short posterior ciliary arteries: Key signalling pathways maintaining physiologic functions. *Sci. Rep.* **6**, 38298 (2016).
59. Chambers, M. C. *et al.* A cross-platform toolkit for mass spectrometry and proteomics. *Nat. Biotechnol.* **30**(10), 918–920 (2012).
60. Demichev, V. *et al.* DIA-NN: Neural networks and interference correction enable deep proteome coverage in high throughput. *Nat. Methods* **17**(1), 41–44 (2020).
61. Tyanova, S. *et al.* The Perseus computational platform for comprehensive analysis of (prote)omics data. *Nat. Methods* **13**(9), 731–740 (2016).
62. Rudolph, J. D. & Cox, J. A network module for the Perseus software for computational proteomics facilitates proteome interaction graph analysis. *J. Proteome Res.* **18**(5), 2052–2064 (2019).
63. Huang, D. W., Sherman, B. T. & Lempicki, R. A. Systematic and integrative analysis of large gene lists using DAVID bioinformatics resources. *Nat. Protoc.* **4**(1), 44–57 (2009).
64. Sherman, B. T. *et al.* DAVID: A web server for functional enrichment analysis and functional annotation of gene lists (2021 update). *Nucleic Acids Res.* **50**(W1), W216–W221 (2022).
65. Kanehisa, M. & Goto, S. KEGG: Kyoto encyclopedia of genes and genomes. *Nucleic Acids Res.* **28**(1), 27–30 (2000).
66. Kanehisa, M. Toward understanding the origin and evolution of cellular organisms. *Protein Sci.* **28**(11), 1947–1951 (2019).
67. Kanehisa, M. *et al.* KEGG for taxonomy-based analysis of pathways and genomes. *Nucleic Acids Res.* **51**(D1), D587–D592 (2023).

Acknowledgements

This work was supported by the Deutsche Forschungsgemeinschaft (DFG) with grant PR1569/1–1 and the large instrument grant INST 1856/71-1 FUGG by the German Research Foundation (DFG Großgeräteantrag). We thank Dr. Valerio Ganci for his assistance in generating some of the figures.

Author contributions

X.W. wrote the main manuscript text, L.F., P.L., X.S. and Y.F. assisted with the experiment. N.N.W. contributed to the analysis. H.L. and V.P. aided in revising the manuscript. All authors reviewed the manuscript.

Funding

Open Access funding enabled and organized by Projekt DEAL.

Competing interests

The authors declare no competing interests.

Additional information

Supplementary Information The online version contains supplementary material available at <https://doi.org/10.1038/s41598-024-72378-z>.

Correspondence and requests for materials should be addressed to V.P.

Reprints and permissions information is available at www.nature.com/reprints.

Publisher's note Springer Nature remains neutral with regard to jurisdictional claims in published maps and institutional affiliations.

Open Access This article is licensed under a Creative Commons Attribution 4.0 International License, which permits use, sharing, adaptation, distribution and reproduction in any medium or format, as long as you give appropriate credit to the original author(s) and the source, provide a link to the Creative Commons licence, and indicate if changes were made. The images or other third party material in this article are included in the article's Creative Commons licence, unless indicated otherwise in a credit line to the material. If material is not included in the article's Creative Commons licence and your intended use is not permitted by statutory regulation or exceeds the permitted use, you will need to obtain permission directly from the copyright holder. To view a copy of this licence, visit <http://creativecommons.org/licenses/by/4.0/>.

© The Author(s) 2024

5. DISCUSSION

5.1 Proteomic Characteristic in Regenerative Retina

In the present study, the pathways identified as playing a most significant role in RGC regeneration include the thyroid hormone signaling pathway, Notch signaling pathway and Wnt signaling pathway. The thyroid hormone pathway interacts with the Wnt [74] and Notch [75] pathways to fine-tune regeneration. These crosstalk mechanisms contribute to a complex regulatory network that coordinates the regenerative response of RGCs to injury or degeneration.

5.1.1 Thyroid Hormone Signaling Pathway

The thyroid hormone pathway plays a significant role in RGC regeneration. Thyroid hormones, primarily triiodothyronine and thyroxine, are known to exert a profound influence on various cellular processes, including proliferation, differentiation, and axonal outgrowth [76, 77]. Several studies have demonstrated the presence of thyroid hormone receptors, such as TR α and TR β , in the retinal tissue, including RGCs [78, 79]. Activation of these receptors has been shown to stimulate neurite outgrowth and axonal regeneration [80], thereby underscoring the potential of thyroid hormones in facilitating RGC regeneration [81]. And our results align with previous studies that have demonstrated the neuroprotective and regenerative effects of thyroid hormones in the nervous system [82, 83].

5.1.2 Wnt and Notch Signaling Pathways

The Notch signaling pathway and the Wnt signaling pathway emerge as additional pivotal KEGG pathways identified within the RGC regeneration groups. More than 50% of the proteins commonly enriched in the current study affirm the existence of cross-talk interactions between these two signaling pathways [84]. Notch signaling is known for its role in regulating cell fate and differentiation and it participates in neurogenesis and gliogenesis [85]. In the context of the retina, its involvement in retinal development and homeostasis has been well-documented [86]. Our results suggest that it is instrumental in guiding RGCs toward a regenerative state. This finding is in line with the growing body of evidence implicating Notch signaling in neuronal regenerative processes [87, 88]. The Wnt pathway's involvement in RGC regeneration is consistent with its established role in cellular proliferation, differentiation and homeostasis as well as axon extension, growth cone guidance and synaptogenesis [89-91]. Several studies have demonstrated that augmenting Wnt pathway activity within RGCs or their microenvironment leads to enhanced axonal regeneration and augmented neuronal survival after optic nerve injury [92, 93].

5.1.3 SIRT1/ CaMKII α / CBP / EP300 as Key Players

The PPI network analysis within pathways has provided valuable insights into the identification of central regulatory elements crucial for orchestrating the regenerative processes in RGCs. Among the numerous proteins investigated, the results of this analysis have underscored the significance of key players, notably SIRT1, CBP, EP300, and CaMKII α .

NAD-dependent protein deacetylase sirtuin-1(SIRT1), a protein implicated in the neuroprotective mechanisms against RGC degeneration in glaucoma, has garnered significant recognition [94-97]. Notably, a reduction in SIRT1 expression has been observed in glaucoma patients [98], and its pivotal role as a central regulator in safeguarding RGCs has been established through both in vivo [96] and in vitro [99] experiments. Activation of SIRT1, especially through the SIRT1/CREB axis [99], has been demonstrated to induce neurite outgrowth, thereby enhancing the regenerative potential of RGCs. In our research, SIRT1 emerged as the most central and influential player within the RGC regeneration context, positioning it as the primary candidate for fostering RGC survival and promoting regeneration. The underlying mechanism involves the enhancement of neuronal autophagy [100, 101] and inhibition of neuronal apoptosis [102] process.

Histone lysine acetyltransferase CREBBP (CBP, CREBBP) and Histone acetyltransferase p300 (EP300, p300) are highly homologous proteins (with >70% of overall identity) and share a substantial overlap in their known functional domains [103, 104]. They are commonly regarded as pivotal "master coactivators" that serve the purpose of stimulating transcription and augmenting gene expression [105]. CBP and EP300 occupy central role in the development of the mammalian eye [106]. Mutations within the CBP or EP300 gene have been identified as the causative factor for Rubenstein-Taybi syndrome, a condition characterized, in part, by various retinal disorders, including glaucoma [105-107]. EP300 inhibition suppressed the neuronal regeneration in zebrafish optic tectum after the injury [108]. CBP-mediated histone acetylation is of paramount significance in facilitating the sustained enhancement of neurite outgrowth and axon regeneration following exposure to environmental enrichment [109]. Moreover, augmenting CBP activity has been observed to promote axon regeneration after injuries in CNS [110]. CBP is equipped with Ca²⁺-sensitive transactivation domains and its pivotal role in neuroplasticity and RGC protection is known to be regulated by calcium ions and calcium/calmodulin-dependent protein kinases, specifically CaMKII [111, 112]. Remarkably, in the present study, our investigation not only identified CBP as one of the most critical effectors in RGC regeneration but also revealed the efficacy of CaMKII α as a contributing factor. CaMKII is recognized as a central coordinator and executor of calcium signal transduction, with responsibilities extending to the regulation of various cellular

processes [113, 114]. Activation of the CaMKII/CBP axis was empirically demonstrated to safeguard long-distance RGC axon projections in vivo, preserving visual function from the retina to the visual cortex, thereby positively impacting visually guided behavior [112]. Our study thus underscores the pivotal roles played by the SIRT1/ CaMKII α / CBP / EP300 network in RGC protection and axon regeneration.

5.2 Proteomic Characteristic in Glaucomatous Degenerative Retina

5.2.1 Pathways of Neurodegeneration

The “pathways of neurodegeneration” exhibited significant enrichment in the degeneration group, with 20 up-regulated proteins implicated. The PPI network analysis identified key players ITPR1, M3K5, CASP9, PPP3R1, CIO72, RBCC1 and ATXN2. ITPR1, M3K5, CASP9, and EIF2AK3 predominantly participate in the intrinsic apoptotic signaling pathway in response to endoplasmic reticulum (ER) stress. CIO72, ATXN2 and ATX2L primarily participate in the formation of cytoplasmic stress granule (SG).

5.2.2 Apoptotic Signaling Pathway in Response to ER Stress

The apoptosis pathway is restricted in mature neurons to ensure their survival [115]. However, mature neurons are still capable of activating the apoptotic pathway in certain pathological contexts [116]. Caspase-9 (CASP9), the initiator protease, has received widespread attention for its indispensable role as a pivotal component within the intrinsic apoptotic pathway, primarily governed by the mitochondria [117]. Mitogen-activated protein kinase kinase kinase 5 (MAP3K5), widely recognized as apoptosis signal-regulating kinase 1 (ASK1) [118], plays a central role. Excessive and sustained activation of these components leads to cell death and is implicated in the development of many neurological disorders, notably including glaucoma [119, 120].

Inositol 1,4,5-trisphosphate receptor type 1 (ITPR1, IP3R1) is resident ER calcium channels that control calcium release from intracellular stores [121] and has been implicated in injury-induced axon degeneration [122]. Neurodegenerative disorders instigate the overexpression of ITPR1, and this modification unfavorably augments the Gq-protein coupled receptor-triggered intracellular Ca²⁺ release [122, 123]. Furthermore, the Ca²⁺ release from the ER counterbalanced by the presence of adjacent mitochondria, culminating in mitochondrial Ca²⁺ overload and consequential dysfunction [122, 123].

5.2.3 Cytoplasmic Stress Granule

The cell component GO term revealed a significant enrichment of the cytoplasmic SG in which several proteins, including ATXN2L, ATXN2, NUFIP2, MCRIP1, KHSRP, PRRC2C, CASC3, LARP4B, PUM1, CIO72, LSM14A, and GIGYF2, were identified. As we mentioned above, among the 20 proteins presenting in the “Pathways of neurodegeneration”, CIO72, ATXN2 and ATX2L participate in the formation of cytoplasmic SG. Notably, all these proteins exhibited upregulation in the degeneration group. SG assembly represents a highly conserved cellular mechanism aimed at mitigating stress-induced damage and promoting cell survival [124].

Neurons respond to stress by transiently forming SGs, but disruptions in SG dynamics can expedite neurodegeneration [124, 125]. Consequently, SGs have been observed in various neurodegenerative conditions, including Alzheimer's disease, amyotrophic lateral sclerosis and front-temporal dementia [124, 125]. Surprisingly, in this study, we identified SGs in a glaucoma model using a bioinformatic approach. Interestingly, a substantial number of proteins implicated in the pathogenesis of these disorders are found within SGs, with the glaucoma-associated protein ATXN2 being a prominent example.

ATXN2 exhibits significant upregulation in our glaucoma model and is notably enriched within cytoplasmic SG and ribonucleoprotein complexes. Its predominant localization within RGCs in ocular and established association with glaucoma underscore its potential role [126, 127]. The RGC degeneration associated with ATXN2 may involve dysregulated Ca^{2+} release from ER stores, presenting intriguing mechanisms in glaucoma pathogenesis [126]. Further research is warranted to elucidate ATXN2 and SGs' precise contributions to glaucomatous processes.

5.2.4 Mitochondrial Functions

Among the 58 down-regulated proteins observed in the RGC degeneration group, 24 exhibit significant enrichment in mitochondrial components and functions, while 7 are notably enriched in mitochondrial respiratory chain complex I which is suggested as the rate-limiting step in overall respiration [128]. This enrichment underscores the pivotal role of mitochondrial dysfunction in the loss of RGCs in glaucoma. Mitochondrial function is crucial for supporting the high metabolic activity and energy demands of RGCs [129, 130]. Impaired mitochondrial function leads to an energy crisis within RGCs, which in turn hinders the activity of Na^+/K^+ ion pumps [130, 131]. This disruption impairs the normal transduction of action potentials along RGC axons [130, 132]. Furthermore, mitochondria serve as a critical battleground for determining cell fate, mediating interactions between anti- and pro-apoptotic factors [130, 133]. When this balance tips toward apoptosis, there is an increase in mitochondrial membrane permeability and the release of various cell death mediators [134], notably CASP9 [130], identified as a central contributor to neurodegeneration in this study.

6. REFERENCES

1. Stein, J.D., A.P. Khawaja, and J.S. Weizer, *Glaucoma in Adults-Screening, Diagnosis, and Management: A Review*. JAMA, 2021. **325**(2): p. 164-174.
2. Tham, Y.C., et al., *Global prevalence of glaucoma and projections of glaucoma burden through 2040: a systematic review and meta-analysis*. Ophthalmology, 2014. **121**(11): p. 2081-90.
3. Strohl, A., et al., *[Secondary glaucoma in Paraguay. Etiology and incidence]*. Ophthalmologie, 1999. **96**(6): p. 359-63.
4. Weinreb, R.N., T. Aung, and F.A. Medeiros, *The pathophysiology and treatment of glaucoma: a review*. JAMA, 2014. **311**(18): p. 1901-11.
5. Montana, C.L. and A.M. Bhorade, *Glaucoma and quality of life: fall and driving risk*. Curr Opin Ophthalmol, 2018. **29**(2): p. 135-140.
6. Pease, M.E., et al., *Obstructed axonal transport of BDNF and its receptor TrkB in experimental glaucoma*. Invest Ophthalmol Vis Sci, 2000. **41**(3): p. 764-74.
7. Hakim, A., et al., *Gene therapy strategies for glaucoma from IOP reduction to retinal neuroprotection: Progress towards non-viral systems*. Adv Drug Deliv Rev, 2023. **196**: p. 114781.
8. Pavlatos, E., et al., *Regional Deformation of the Optic Nerve Head and Peripapillary Sclera During IOP Elevation*. Invest Ophthalmol Vis Sci, 2018. **59**(8): p. 3779-3788.
9. Girkin, C.A., et al., *Retinal electrophysiologic response to IOP elevation in living human eyes*. Exp Eye Res, 2023. **229**: p. 109420.
10. Galassi, F., B. Giambene, and R. Varriale, *Systemic vascular dysregulation and retrobulbar hemodynamics in normal-tension glaucoma*. Invest Ophthalmol Vis Sci, 2011. **52**(7): p. 4467-71.
11. Plange, N., et al., *Prolonged retinal arteriovenous passage time is correlated to ocular perfusion pressure in normal tension glaucoma*. Graefes Arch Clin Exp Ophthalmol, 2008. **246**(8): p. 1147-52.
12. Levine, R.M., et al., *Management of Blood Pressure in Patients with Glaucoma*. Curr Cardiol Rep, 2017. **19**(11): p. 109.
13. Harada, T., et al., *The potential role of glutamate transporters in the pathogenesis of normal tension glaucoma*. J Clin Invest, 2007. **117**(7): p. 1763-70.
14. Sato, M., et al., *Sex differences in the association between systemic oxidative stress status and optic nerve head blood flow in normal-tension glaucoma*. PLoS One, 2023. **18**(2): p. e0282047.
15. Ju, W.K., et al., *Glaucomatous optic neuropathy: Mitochondrial dynamics, dysfunction and protection in retinal ganglion cells*. Prog Retin Eye Res, 2023. **95**: p. 101136.
16. Pan, L., et al., *IGFBPL1 is a master driver of microglia homeostasis and resolution of neuroinflammation in glaucoma and brain tauopathy*. Cell Rep, 2023. **42**(8): p. 112889.
17. Wang, R. and J.L. Wiggs, *Common and rare genetic risk factors for glaucoma*. Cold Spring Harb Perspect Med, 2014. **4**(12): p. a017244.
18. Sakurada, Y. and F. Mabuchi, *Genetic Risk Factors for Glaucoma and Exfoliation Syndrome Identified by Genome-wide Association Studies*. Curr Neuropharmacol, 2018. **16**(7): p. 933-941.
19. Chae, B., T. Cakiner-Egilmez, and M. Desai, *Glaucoma medications*. Insight, 2013. **38**(1): p. 5-9; quiz 10.
20. Jayaram, H., et al., *Glaucoma: now and beyond*. Lancet, 2023. **402**(10414): p. 1788-1801.
21. Storgaard, L., et al., *Glaucoma Clinical Research: Trends in Treatment Strategies and Drug Development*. Front Med (Lausanne), 2021. **8**: p. 733080.
22. Nagstrup, A.H., *The use of benzalkonium chloride in topical glaucoma treatment: An investigation of the efficacy and safety of benzalkonium chloride-preserved intraocular pressure-lowering eye drops and their effect on conjunctival goblet cells*. Acta Ophthalmol, 2023. **101 Suppl 278**: p. 3-21.

23. Gazzard, G., et al., *Laser in Glaucoma and Ocular Hypertension (LiGHT) Trial: Six-Year Results of Primary Selective Laser Trabeculoplasty versus Eye Drops for the Treatment of Glaucoma and Ocular Hypertension*. *Ophthalmology*, 2023. **130**(2): p. 139-151.
24. Gittinger, J.W., Jr., *Management of normal tension glaucoma*. *Surv Ophthalmol*, 2019. **64**(1): p. 101.
25. Miao, Y., et al., *Activation of retinal glial cells contributes to the degeneration of ganglion cells in experimental glaucoma*. *Prog Retin Eye Res*, 2023. **93**: p. 101169.
26. London, A., I. Benhar, and M. Schwartz, *The retina as a window to the brain-from eye research to CNS disorders*. *Nat Rev Neurol*, 2013. **9**(1): p. 44-53.
27. Centanin, L. and J. Wittbrodt, *Retinal neurogenesis*. *Development*, 2014. **141**(2): p. 241-4.
28. Qin, S., Y. Zou, and C.L. Zhang, *Cross-talk between KLF4 and STAT3 regulates axon regeneration*. *Nat Commun*, 2013. **4**: p. 2633.
29. Boyd, J.G. and T. Gordon, *Neurotrophic factors and their receptors in axonal regeneration and functional recovery after peripheral nerve injury*. *Mol Neurobiol*, 2003. **27**(3): p. 277-324.
30. Lindner, R., R. Puttagunta, and S. Di Giovanni, *Epigenetic regulation of axon outgrowth and regeneration in CNS injury: the first steps forward*. *Neurotherapeutics*, 2013. **10**(4): p. 771-81.
31. Tedeschi, A., et al., *A p53-CBP/p300 transcription module is required for GAP-43 expression, axon outgrowth, and regeneration*. *Cell Death Differ*, 2009. **16**(4): p. 543-54.
32. Santos, D., et al., *Preferential Enhancement of Sensory and Motor Axon Regeneration by Combining Extracellular Matrix Components with Neurotrophic Factors*. *Int J Mol Sci*, 2016. **18**(1).
33. Anderson, M.A., et al., *Astrocyte scar formation aids central nervous system axon regeneration*. *Nature*, 2016. **532**(7598): p. 195-200.
34. Blackmore, M.G., et al., *Kruppel-like Factor 7 engineered for transcriptional activation promotes axon regeneration in the adult corticospinal tract*. *Proc Natl Acad Sci U S A*, 2012. **109**(19): p. 7517-22.
35. Norsworthy, M.W., et al., *Sox11 Expression Promotes Regeneration of Some Retinal Ganglion Cell Types but Kills Others*. *Neuron*, 2017. **94**(6): p. 1112-1120 e4.
36. Mason, M.R.J., et al., *The Jun-dependent axon regeneration gene program: Jun promotes regeneration over plasticity*. *Hum Mol Genet*, 2022. **31**(8): p. 1242-1262.
37. Chen, H., et al., *Combined Catalpol and Tetramethylpyrazine Promote Axonal Plasticity in Alzheimer's Disease by Inducing Astrocytes to Secrete Exosomes Carrying CDK5 mRNA and Regulating STAT3 Phosphorylation*. *Mol Neurobiol*, 2024. **61**(12): p. 10770-10791.
38. Ding, Y. and Q. Chen, *mTOR pathway: A potential therapeutic target for spinal cord injury*. *Biomed Pharmacother*, 2022. **145**: p. 112430.
39. Park, K.K., et al., *Promoting axon regeneration in the adult CNS by modulation of the PTEN/mTOR pathway*. *Science*, 2008. **322**(5903): p. 963-6.
40. Huang, H., et al., *PI3K/Akt and ERK/MAPK Signaling Promote Different Aspects of Neuron Survival and Axonal Regrowth Following Rat Facial Nerve Axotomy*. *Neurochem Res*, 2017. **42**(12): p. 3515-3524.
41. Liao, K.K., et al., *Curcuminoids promote neurite outgrowth in PC12 cells through MAPK/ERK- and PKC-dependent pathways*. *J Agric Food Chem*, 2012. **60**(1): p. 433-43.
42. Cheng, Y., et al., *Epigenetic and epitranscriptomic regulation of axon regeneration*. *Mol Psychiatry*, 2023. **28**(4): p. 1440-1450.
43. Muller, F., et al., *CBP/p300 activation promotes axon growth, sprouting, and synaptic plasticity in chronic experimental spinal cord injury with severe disability*. *PLoS Biol*, 2022. **20**(9): p. e3001310.
44. Lu, Y., et al., *Reprogramming to recover youthful epigenetic information and restore vision*. *Nature*, 2020. **588**(7836): p. 124-129.

45. Brugger, V., et al., *Delaying histone deacetylase response to injury accelerates conversion into repair Schwann cells and nerve regeneration*. Nat Commun, 2017. **8**: p. 14272.
46. Blochl, A. and R. Blochl, *A cell-biological model of p75NTR signaling*. J Neurochem, 2007. **102**(2): p. 289-305.
47. Huang, E.J. and L.F. Reichardt, *Trk receptors: roles in neuronal signal transduction*. Annu Rev Biochem, 2003. **72**: p. 609-42.
48. Wood, M.D., et al., *Fibrin matrices with affinity-based delivery systems and neurotrophic factors promote functional nerve regeneration*. Biotechnol Bioeng, 2010. **106**(6): p. 970-9.
49. Laughter, M.R., et al., *Injectable Neurotrophic Factor Delivery System Supporting Retinal Ganglion Cell Survival and Regeneration Following Optic Nerve Crush*. ACS Biomater Sci Eng, 2018. **4**(9): p. 3374-3383.
50. Wang, X., et al., *Driving axon regeneration by orchestrating neuronal and non-neuronal innate immune responses via the IFNgamma-cGAS-STING axis*. Neuron, 2023. **111**(2): p. 236-255 e7.
51. Blanco, R.E., et al., *Application of CNTF or FGF-2 increases the number of M2-like macrophages after optic nerve injury in adult Rana pipiens*. PLoS One, 2019. **14**(5): p. e0209733.
52. Shen, H., et al., *A DAMP-scavenging, IL-10-releasing hydrogel promotes neural regeneration and motor function recovery after spinal cord injury*. Biomaterials, 2022. **280**: p. 121279.
53. Kwon, M.J., et al., *CCL2 Mediates Neuron-Macrophage Interactions to Drive Proregenerative Macrophage Activation Following Preconditioning Injury*. J Neurosci, 2015. **35**(48): p. 15934-47.
54. Nocera, G. and C. Jacob, *Mechanisms of Schwann cell plasticity involved in peripheral nerve repair after injury*. Cell Mol Life Sci, 2020. **77**(20): p. 3977-3989.
55. Wang, X., et al., *Comparative proteomic analysis of regenerative mechanisms in mouse retina to identify markers for neuro-regeneration in glaucoma*. Sci Rep, 2024. **14**(1): p. 23118.
56. Hanash, S., *Disease proteomics*. Nature, 2003. **422**(6928): p. 226-32.
57. Li, X., W. Wang, and J. Chen, *Recent progress in mass spectrometry proteomics for biomedical research*. Sci China Life Sci, 2017. **60**(10): p. 1093-1113.
58. Goldberg, J.L., et al., *Amacrine-signaled loss of intrinsic axon growth ability by retinal ganglion cells*. Science, 2002. **296**(5574): p. 1860-4.
59. Fischer, D., P. Heiduschka, and S. Thanos, *Lens-injury-stimulated axonal regeneration throughout the optic pathway of adult rats*. Exp Neurol, 2001. **172**(2): p. 257-72.
60. Shuken, S.R., *An Introduction to Mass Spectrometry-Based Proteomics*. J Proteome Res, 2023. **22**(7): p. 2151-2171.
61. Rabilloud, T., et al., *Two-dimensional gel electrophoresis in proteomics: Past, present and future*. J Proteomics, 2010. **73**(11): p. 2064-77.
62. Zhang, Z., et al., *High-throughput proteomics*. Annu Rev Anal Chem (Palo Alto Calif), 2014. **7**: p. 427-54.
63. Fernandez-Costa, C., et al., *Impact of the Identification Strategy on the Reproducibility of the DDA and DIA Results*. J Proteome Res, 2020. **19**(8): p. 3153-3161.
64. Lu, L., et al., *Mesh Fragmentation Improves Dissociation Efficiency in Top-down Proteomics*. J Am Soc Mass Spectrom, 2021. **32**(6): p. 1319-1325.
65. Hu, W., et al., *GlycoPep MassList: software to generate massive inclusion lists for glycopeptide analyses*. Anal Bioanal Chem, 2017. **409**(2): p. 561-570.
66. Li, W., et al., *Assessing the Relationship Between Mass Window Width and Retention Time Scheduling on Protein Coverage for Data-Independent Acquisition*. J Am Soc Mass Spectrom, 2019. **30**(8): p. 1396-1405.
67. Zhong, X., et al., *Mass Defect-Based DiLeu Tagging for Multiplexed Data-Independent Acquisition*. Anal Chem, 2020. **92**(16): p. 11119-11126.

68. Fu, Q., et al., *A Proteomics Pipeline for Generating Clinical Grade Biomarker Candidates from Data-Independent Acquisition Mass Spectrometry (DIA-MS) Discovery*. *Angew Chem Int Ed Engl*, 2024. **63**(52): p. e202409446.
69. Sun, R., et al., *Proteomic landscape profiling of primary prostate cancer reveals a 16-protein panel for prognosis prediction*. *Cell Rep Med*, 2024. **5**(8): p. 101679.
70. Dozio, V. and J.C. Sanchez, *Profiling the proteomic inflammatory state of human astrocytes using DIA mass spectrometry*. *J Neuroinflammation*, 2018. **15**(1): p. 331.
71. Wu, L., et al., *Cross-sectional study of proteomic differences between moderate and severe psoriasis*. *Sci Rep*, 2025. **15**(1): p. 3387.
72. Wei, Y., et al., *Progress in multi-omics studies of osteoarthritis*. *Biomark Res*, 2025. **13**(1): p. 26.
73. Ke, C., et al., *Genetic and Plasma Proteomic Approaches to Identify Therapeutic Targets for Graves' Disease and Graves' Ophthalmopathy*. *Immunotargets Ther*, 2025. **14**: p. 87-98.
74. Skah, S., et al., *The thyroid hormone nuclear receptors and the Wnt/beta-catenin pathway: An intriguing liaison*. *Dev Biol*, 2017. **422**(2): p. 71-82.
75. Hasebe, T., et al., *Thyroid Hormone-Induced Activation of Notch Signaling is Required for Adult Intestinal Stem Cell Development During *Xenopus Laevis* Metamorphosis*. *Stem Cells*, 2017. **35**(4): p. 1028-1039.
76. Rosato-Siri, M.V., et al., *Combination therapy of apo-transferrin and thyroid hormones enhances remyelination*. *Glia*, 2021. **69**(1): p. 151-164.
77. Kormpakis, I., et al., *Silicone tubes with thyroid hormone (Tau3) and BDNF as an alternative to autografts for bridging neural defects*. *Injury*, 2020. **51**(12): p. 2879-2886.
78. Arbogast, P., et al., *Thyroid Hormone Signaling in the Mouse Retina*. *PLoS One*, 2016. **11**(12): p. e0168003.
79. Ng, L., et al., *Biphasic expression of thyroid hormone receptor TRbeta1 in mammalian retina and anterior ocular tissues*. *Front Endocrinol (Lausanne)*, 2023. **14**: p. 1174600.
80. Faustino, L.C. and T.M. Ortega-Carvalho, *Thyroid hormone role on cerebellar development and maintenance: a perspective based on transgenic mouse models*. *Front Endocrinol (Lausanne)*, 2014. **5**: p. 75.
81. Nakagawa, S., et al., *Ephrin-B regulates the Ipsilateral routing of retinal axons at the optic chiasm*. *Neuron*, 2000. **25**(3): p. 599-610.
82. Baldassarro, V.A., et al., *Neuroprotection and neuroregeneration: roles for the white matter*. *Neural Regen Res*, 2022. **17**(11): p. 2376-2380.
83. Breton, J.M., et al., *Hormonal Regulation of Oligodendrogenesis II: Implications for Myelin Repair*. *Biomolecules*, 2021. **11**(2).
84. Mills, E.A. and D. Goldman, *The Regulation of Notch Signaling in Retinal Development and Regeneration*. *Curr Pathobiol Rep*, 2017. **5**(4): p. 323-331.
85. Traiffort, E. and J. Ferent, *[Neural stem cells and Notch signalling]*. *Med Sci (Paris)*, 2015. **31**(12): p. 1115-25.
86. Zheng, M., et al., *The Notch signaling pathway in retinal dysplasia and retina vascular homeostasis*. *J Genet Genomics*, 2010. **37**(9): p. 573-82.
87. Wang, X., et al., *Loss of *ndrg2* Function Is Involved in Notch Activation in Neuromast Hair Cell Regeneration in Zebrafish*. *Mol Neurobiol*, 2023. **60**(6): p. 3100-3112.
88. Davis, C.K. and K.R. G., *Postischemic supplementation of folic acid improves neuronal survival and regeneration in vitro*. *Nutr Res*, 2020. **75**: p. 1-14.
89. Xiao, Q., et al., *The many postures of noncanonical Wnt signaling in development and diseases*. *Biomed Pharmacother*, 2017. **93**: p. 359-369.
90. Garcia, A.L., et al., *A growing field: The regulation of axonal regeneration by Wnt signaling*. *Neural Regen Res*, 2018. **13**(1): p. 43-52.
91. Cheng, P., H.Y. Liao, and H.H. Zhang, *The role of Wnt/mTOR signaling in spinal cord injury*. *J Clin Orthop Trauma*, 2022. **25**: p. 101760.
92. Musada, G.R., T. Carmy-Bennun, and A.S. Hackam, *Identification of a Novel Axon Regeneration Role for Noncanonical Wnt Signaling in the Adult Retina after Injury*. *eNeuro*, 2022. **9**(4).

93. Patel, A.K., K.K. Park, and A.S. Hackam, *Wnt signaling promotes axonal regeneration following optic nerve injury in the mouse*. Neuroscience, 2017. **343**: p. 372-383.
94. Munemasa, Y. and Y. Kitaoka, *Autophagy in axonal degeneration in glaucomatous optic neuropathy*. Prog Retin Eye Res, 2015. **47**: p. 1-18.
95. Yue, J., et al., *Cell-Specific Expression of Human SIRT1 by Gene Therapy Reduces Retinal Ganglion Cell Loss Induced by Elevated Intraocular Pressure*. Neurotherapeutics, 2023. **20**(3): p. 896-907.
96. Zuo, L., et al., *SIRT1 promotes RGC survival and delays loss of function following optic nerve crush*. Invest Ophthalmol Vis Sci, 2013. **54**(7): p. 5097-102.
97. Bai, X., et al., *Neuroprotection of SRT2104 in Murine Ischemia/Reperfusion Injury Through the Enhancement of Sirt1-Mediated Deacetylation*. Invest Ophthalmol Vis Sci, 2023. **64**(4): p. 31.
98. Yaman, D., et al., *Evaluation of silent information regulator T (SIRT) 1 and Forkhead Box O (FOXO) transcription factor 1 and 3a genes in glaucoma*. Mol Biol Rep, 2020. **47**(12): p. 9337-9344.
99. Zhao, N., et al., *The Combination of Citicoline and Nicotinamide Mononucleotide Induces Neurite Outgrowth and Mitigates Vascular Cognitive Impairment via SIRT1/CREB Pathway*. Cell Mol Neurobiol, 2023. **43**(8): p. 4261-4277.
100. Kitaoka, Y., et al., *Axonal protection by a small molecule SIRT1 activator, SRT2104, with alteration of autophagy in TNF-induced optic nerve degeneration*. Jpn J Ophthalmol, 2020. **64**(3): p. 298-303.
101. Kitaoka, Y. and K. Sase, *Molecular aspects of optic nerve autophagy in glaucoma*. Mol Aspects Med, 2023. **94**: p. 101217.
102. Hu, C., et al., *Melatonin prevents EAAC1 deletion-induced retinal ganglion cell degeneration by inhibiting apoptosis and senescence*. J Pineal Res, 2024. **76**(1): p. e12916.
103. Valor, L.M., et al., *Lysine acetyltransferases CBP and p300 as therapeutic targets in cognitive and neurodegenerative disorders*. Curr Pharm Des, 2013. **19**(28): p. 5051-64.
104. Chan, H.M. and N.B. La Thangue, *p300/CBP proteins: HATs for transcriptional bridges and scaffolds*. J Cell Sci, 2001. **114**(Pt 13): p. 2363-73.
105. de Thonel, A., et al., *CBP-HSF2 structural and functional interplay in Rubinstein-Taybi neurodevelopmental disorder*. Nat Commun, 2022. **13**(1): p. 7002.
106. Anderson, J., R. Bhandari, and J.P. Kumar, *A genetic screen identifies putative targets and binding partners of CREB-binding protein in the developing Drosophila eye*. Genetics, 2005. **171**(4): p. 1655-72.
107. Enomoto, Y., et al., *Divergent variant patterns among 19 patients with Rubinstein-Taybi syndrome uncovered by comprehensive genetic analysis including whole genome sequencing*. Clin Genet, 2022. **101**(3): p. 335-345.
108. Shimizu, Y. and T. Kawasaki, *Histone acetyltransferase EP300 regulates the proliferation and differentiation of neural stem cells during adult neurogenesis and regenerative neurogenesis in the zebrafish optic tectum*. Neurosci Lett, 2021. **756**: p. 135978.
109. Hutson, T.H., et al., *Cbp-dependent histone acetylation mediates axon regeneration induced by environmental enrichment in rodent spinal cord injury models*. Sci Transl Med, 2019. **11**(487).
110. Tang, B.L., *Axon regeneration induced by environmental enrichment- epigenetic mechanisms*. Neural Regen Res, 2020. **15**(1): p. 10-15.
111. Hu, S.C., J. Chrivia, and A. Ghosh, *Regulation of CBP-mediated transcription by neuronal calcium signaling*. Neuron, 1999. **22**(4): p. 799-808.
112. Guo, X., et al., *Preservation of vision after CaMKII-mediated protection of retinal ganglion cells*. Cell, 2021. **184**(16): p. 4299-4314 e12.
113. Hudmon, A. and H. Schulman, *Neuronal CA2+/calmodulin-dependent protein kinase II: the role of structure and autoregulation in cellular function*. Annu Rev Biochem, 2002. **71**: p. 473-510.
114. Berridge, M.J., P. Lipp, and M.D. Bootman, *The versatility and universality of calcium signalling*. Nat Rev Mol Cell Biol, 2000. **1**(1): p. 11-21.

115. Kole, A.J., R.P. Annis, and M. Deshmukh, *Mature neurons: equipped for survival*. Cell Death Dis, 2013. **4**(6): p. e689.
116. Hollville, E., S.E. Romero, and M. Deshmukh, *Apoptotic cell death regulation in neurons*. FEBS J, 2019. **286**(17): p. 3276-3298.
117. Johnson, C.R. and W.D. Jarvis, *Caspase-9 regulation: an update*. Apoptosis, 2004. **9**(4): p. 423-7.
118. Ogier, J.M., B.A. Nayagam, and P.J. Lockhart, *ASK1 inhibition: a therapeutic strategy with multi-system benefits*. J Mol Med (Berl), 2020. **98**(3): p. 335-348.
119. Obsilova, V., K. Honzejkova, and T. Obsil, *Structural Insights Support Targeting ASK1 Kinase for Therapeutic Interventions*. Int J Mol Sci, 2021. **22**(24).
120. Lamoke, F., et al., *Loss of thioredoxin function in retinas of mice overexpressing amyloid beta*. Free Radic Biol Med, 2012. **53**(3): p. 577-88.
121. Pease-Raissi, S.E., et al., *Paclitaxel Reduces Axonal Bclw to Initiate IP(3)R1-Dependent Axon Degeneration*. Neuron, 2017. **96**(2): p. 373-386 e6.
122. Villegas, R., et al., *Calcium release from intra-axonal endoplasmic reticulum leads to axon degeneration through mitochondrial dysfunction*. J Neurosci, 2014. **34**(21): p. 7179-89.
123. Tiscione, S.A., et al., *IP(3)R-driven increases in mitochondrial Ca(2+) promote neuronal death in NPC disease*. Proc Natl Acad Sci U S A, 2021. **118**(40).
124. Mahboubi, H. and U. Stochaj, *Cytoplasmic stress granules: Dynamic modulators of cell signaling and disease*. Biochim Biophys Acta Mol Basis Dis, 2017. **1863**(4): p. 884-895.
125. Kassouf, T., et al., *Targeting the NEDP1 enzyme to ameliorate ALS phenotypes through stress granule disassembly*. Sci Adv, 2023. **9**(13): p. eabq7585.
126. Sundberg, C.A., et al., *The RNA-binding protein and stress granule component ATAXIN-2 is expressed in mouse and human tissues associated with glaucoma pathogenesis*. J Comp Neurol, 2022. **530**(2): p. 537-552.
127. Bailey, J.N., et al., *Genome-wide association analysis identifies TXNRD2, ATXN2 and FOXC1 as susceptibility loci for primary open-angle glaucoma*. Nat Genet, 2016. **48**(2): p. 189-94.
128. Sharma, L.K., J. Lu, and Y. Bai, *Mitochondrial respiratory complex I: structure, function and implication in human diseases*. Curr Med Chem, 2009. **16**(10): p. 1266-77.
129. Wang, L., et al., *Varicosities of intraretinal ganglion cell axons in human and nonhuman primates*. Invest Ophthalmol Vis Sci, 2003. **44**(1): p. 2-9.
130. Almasieh, M., et al., *The molecular basis of retinal ganglion cell death in glaucoma*. Prog Retin Eye Res, 2012. **31**(2): p. 152-81.
131. Ames, A., 3rd, et al., *Energy metabolism of rabbit retina as related to function: high cost of Na⁺ transport*. J Neurosci, 1992. **12**(3): p. 840-53.
132. Ames, A., 3rd, *CNS energy metabolism as related to function*. Brain Res Brain Res Rev, 2000. **34**(1-2): p. 42-68.
133. Armstrong, J.S., *Mitochondrial membrane permeabilization: the sine qua non for cell death*. Bioessays, 2006. **28**(3): p. 253-60.
134. Scaffidi, C., et al., *Two CD95 (APO-1/Fas) signaling pathways*. EMBO J, 1998. **17**(6): p. 1675-87.

7. PRE-PUBLICATIONS OF RESULTS

1. Wang X, Fröhn L, Li P, et al. Comparative proteomic analysis of regenerative mechanisms in mouse retina to identify markers for neuro-regeneration in glaucoma[J]. Scientific Reports, 2024, 14(1): 23118.

This Cumulative thesis includes the paper of No. 1.